SKB

TECHNICAL REPORT 89-05

SKB WP-Cave Project
Transport of escaping radionuclides from the WP-Cave repository to the biosphere

Luis Moreno, Sue Arve, Ivars Neretnieks

Royal Institute of Technology, Stockholm, Sweden

June 1989

SVENSK KÄRNBRÄNSLEHANTERING AB
SWEDISH NUCLEAR FUEL AND WASTE MANAGEMENT CO

BOX 5864 S-102 48 STOCKHOLM
TEL 08-665 28 00 TELEX 13108-SKB

SKB-WP-CAVE PROJECT
TRANSPORT OF ESCAPING RADIONUCLIDES FROM THE WP-CAVE REPOSITORY TO THE BIOSPHERE

Luis Moreno, Sue Arve, Ivars Neretnieks

Royal Institute of Technology, Stockholm, Sweden

June 1989

SKB-WP-CAVE PROJECT

TRANSPORT OF ESCAPING RADIONUCLIDES FROM THE WP-CAVE REPOSITORY TO THE BIOSPHERE

Luis Moreno
Sue Arve
Ivars Neretnieks

Royal Institute of Technology
S-100 44 Stockholm, Sweden

June, 1989

KAT 88/30

ABSTRACT

Far-field release rates for radionuclides that have escaped from the WP-Cave repository (excluding the surrounding hydraulic cage) are calculated using the channeling model. The model considers flow in channels with different flowrates. The channeling model is based on the assumption that the channels are independent over a certain distance. In each channel the model takes into account the advective transport of the nuclide along a fracture with dispersion in the fracture and diffusion and sorption in the rock matrix. Preliminary calculations are performed to determine which parameters influence the release rate of the nuclides from the repository. These parameters are the travel length, channel width, and flowrate. The final results show that most of the radionuclides are not retarded to any great extent (if any) in the surrounding rock. The nuclides that are retarded in the rock are those that have a high sorption coefficient and/or short half-life. The calculations are performed for fractures that are 1 m in width, travel distance of 100 m and a flowrate of 0.3 l/m^2a.

TABLE OF CONTENTS

SUMMARY

Escaping radionuclides from the WP-Cave repository to the biosphere are modeled with a simple model based on the assumption that the channels are independent over a certain distance. The model calculations show that the few fast channels with little sorption area may carry sorbing radionuclides at a rate which may not let the radionuclides decay as well as they would if the rock were more, and more evenly fractured. The proposed hydraulic cage surrounding the repository has been neglected in the calculations presented in this report.

Data on the channel frequency and flow distribution in the surrounding rock are taken from the SFR repository site. The flowrate used in the calculations is obtained from a survey of site areas at different depths around Sweden.

Sample calculations for three nuclides, ^{94}Nb, ^{99}Tc, and ^{129}I, are performed based on their representation of no sorption to high sorption characteristics in granitic rock to illustrate which parameters are of importance.

Far-field release rates are calculated for fission product radionuclides that have escaped the sand-bentonite barrier surrounding the repository. Conclusions drawn from the results indicate that the radionuclides are not retarded to any great extent in the surrounding rock for a travel distance of 100 meters.

Release from the far-field to the biosphere for ^{242}Pu and for the radionuclides in four chains are also calculated. Results show that the maximum release is reduced to about 50 % of the release from the near-field for a transport distance of 100 m. Larger transport distances significantly reduce the release. The low solubility of the actinides under reducing conditions, which exist outside the canister, may reduce the release by some orders of magnitude. The influence of oxidizing conditions in the far-field is also investigated. In this case the effect of the far-field as a barrier is negligible.

Dose rates are also calculated for different scenarios.

1 BACKGROUND, INTRODUCTION, AND STRUCTURE OF REPORT

1.1 BACKGROUND AND INTRODUCTION

One proposal of storing high-level nuclear waste is in the WP-Cave. The WP-Cave is an egg-shaped underground repository surrounded by two engineered barriers: a 5 m thick sand-bentonite layer and a hydraulic cage. The purpose of the hydraulic cage is to divert any passing groundwater away from the repository so that it will not penetrate through the repository. In time, radionuclides will eventually escape from the repository's storage canisters due to canister failure. These nuclides will dissolve into the surrounding water and then migrate into the rock mass and sand-bentonite barrier surrounding the repository. Those radionuclides not retained by the sand-bentonite barrier will be transported to the biosphere by the water flowing in fractures in the rock.

Since no specific site has yet been chosen for the WP-Cave repository, no information of water channeling in the rock is available. Therefore to assess the radionuclide transport in the geosphere, the observations from the SFR repository are used in this report. At the SFR site, a detailed mapping of all wet spots was performed and it showed that the water flows in sparse isolated spots from the walls of the drift. This has been taken as an indication that there may be flow in isolated narrow channels with limited contact surface between the mobile water and the rock which may give only little surface for the sorbing nuclides to sorb on.

In this report a channeling model is used to calculate the radionuclides migration in the rock. The results are compared with the conventional Advection-Dispersion-matrix diffusion model using channels of similar properties.

1.2 STRUCTURE OF REPORT

We first describe the flow system observed at the SFR site and give the reasons for choosing a channeling model to describe the radionuclide migration. The model is then described both conceptually and in mathematical form and the relation of this model to the conventional Advection-Dispersion type of approach is discussed briefly. The data used in the model calculations and a central case defined for three nuclides which represent extreme properties are then given. The properties of the model are explored by sample calculations with the three selected nuclides and the impact of the parameter values is also explored. The results from these selected sample calculations indicate the sensitivity of the system to various parameters and assumptions. The model is then used to calculate the transport through and release from the "geosphere" of ten nuclides that are released from the sand-bentonite layer of the WP-Cave repository. Release rates from the far-field for radionuclides which are members of decaying chains are also calculated. The results of the calculations and the applicability of data are then discussed.

2 DESCRIPTION OF THE FLOW SYSTEM AND CHANNEL OBSERVATIONS

The transport of solutes in fractured rock has often been modeled as taking place in a porous medium. Recent observations in the field indicate that the flow may be concentrated to preferential sparse pathways. This influences the solute transport in at least two important ways. A few preferential paths will give the solutes less rock surface to interact with than if the fluid were to flow in all (or most) of the fractures. Retardation will be less.

The other effect is that mixing between fast and slow paths may not be very frequent and the fast channels will not dilute their waters by mixing with the slow channels.

With the present less than full understanding of the flow system, the case where there are sparse preferential pathways is more conservative and we will therefore use this as the basis for our calculations.

The observations underlying our model are discussed in some detail, the model is described and comparisons with a "porous medium" or frequent mixing model are discussed. Also a discussion on the applicability of the present model and the difficulties of interpreting field observations are made.

2.1 OBSERVATIONS AT SFR

Bolvede and Christiansson /1987/ made a detailed survey of the water flow in the rock in the SFR drifts and tunnels. It was found that under the prevailing hydraulic gradient, the ceilings of the four main repository tunnels have a water inflow of 30 l/min. This flowrate emerged from 164 different spots. 41 of the spots are at fracture intersections or small holes (points). The total area of observation in these tunnels was 14,000 m^2.

The flowrates in the different spots at SFR were measured and grouped in six different ranges. These results are shown in Table 2-1 and Figures 2-1 and 2-2. Table 2-1 shows that nearly 50 % of the flowrate can be accounted for in 18 spots over an area of 14,000 m^2.

Table 2-1 Summary of the flowrates in different flowrate ranges in the four main tunnels of SFR.

Flowrate range l/min	Number of spots	Flowrate l/min	Fraction of spots	Fraction of flow	Flow per spot l/min
<0.1	67	2.53	0.409	0.083	0.038
0.1-<0.2	38	3.85	0.232	0.126	0.101
0.2-<0.4	41	9.30	0.250	0.305	0.227
0.4-<0.8	12	6.30	0.073	0.207	0.525
0.8-<1.6	4	4.50	0.024	0.148	1.125
>=1.6	2	4.00	0.012	0.131	2.000
Total	164	30.48	1.00	1.00	

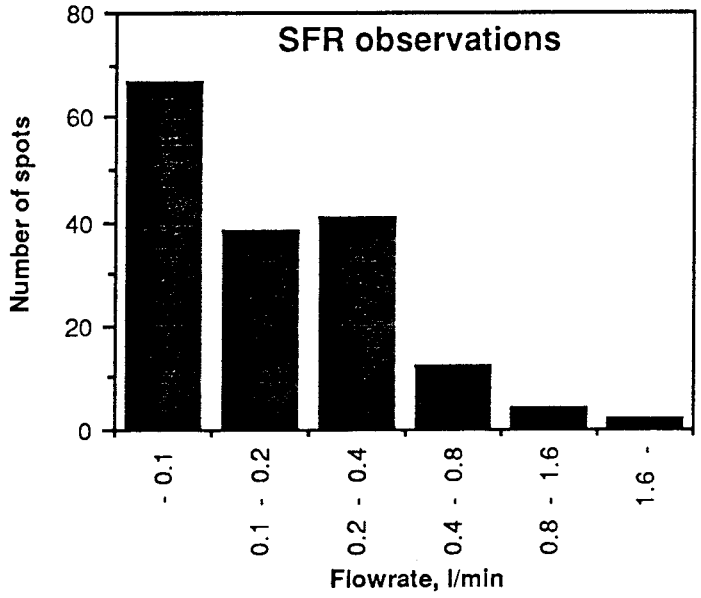

Figure 2-1 Number of spots carrying different ranges of flow in the four main tunnels of SFR.

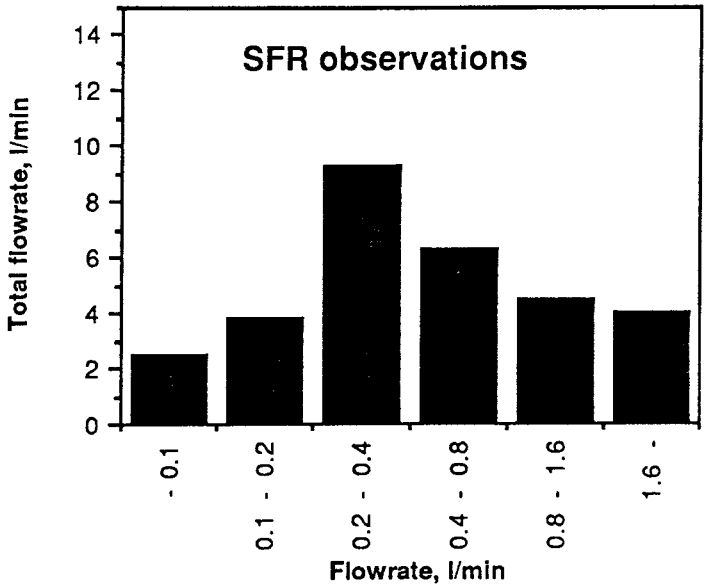

Figure 2-2 Sum of flowrates in the different flowrate ranges in the four main tunnels of SFR.

Interpretations of the observations from the SFR flowrates conclude that on the average there is only one channel per 85 m^2 at SFR. Of these channels, a few carry most of the water. 50 % of the flow takes place in less than 10 % of the channels. It was noted that many of the channels with the highest flowrates were very narrow. The water emerged essentially in a small point in the rock. The wetted surface of the channels per volume of rock is very small if only those channels which carry most of the water are accounted for in this case.

2.2 OBSERVATIONS IN THE KYMMEN TUNNEL

The Kymmen tunnel is a full face drilled tunnel, 4.6 m in diameter. The tunnel transports water to a hydroelectric power plant. A detailed survey of the Kymmen tunnel has been made by Palmqvist and Stanfors /1987/. The observations are summarized in Table 2-2. The tunnel has a length of 4500 m and traverses four major rock types: Gneiss-granite (Gg) 13 % of length, Gneiss-granite with slabs of Amphibolite (GgA) 40 %, fine grained quartz-porfyres called Leptite (L) 40 %, and Amphibolite (A) 7 %.

Table 2-2 Number of spots in Kymmen divided according to rock type. Number of spots per 100 m tunnel.

Rock	length of tunnel,m	Flow range l/min 0.01-0.2	0.2-1.5	1.5-6.5	>6.5
Gg	640	1.7	0.8	-	-
GgA	1891	3.6	1.8	0.2	-
L	1896	8.6	5.0	0.2	0.2
A	69	-	2.9	-	-

The different leak spots have been characterized. The clear majority of the leaks with a flowrate larger than 0.2 l/min (368 leaks) have very small extent and they are called point leaks. Only 29 leaks have an extent larger than 0.2 m. In addition there is a large number of spots with flow less than 0.01 l/min and some diffuse wet areas but these account for only a small fraction of the total flowrate. The density of wet spots is one spot per 163 m^2

2.3 OBSERVATIONS AT STRIPA

In Stripa 3D experiment /Neretnieks et al., 1987/, a 75 m long drift was excavated at 360 m below the ground level. The drift was covered with more than 375 individual plastic sheets, and the natural water flowrate was monitored for nearly 3 years. It was found that the flowrate varied considerably between different areas and between different sheets in the different areas. On this scale at least there was a strong concentration of flow in some areas, whereas other areas were dry or had very small flowrates. Table 2-3 shows the flowrate distribution among the 375 sheets in the drift. It can be seen in Table 2-3 that 50 % of the flow takes place in about 3 % of all the covered area.

Table 2-3 The distribution of flowrates in the Stripa 3D drift among the 375 sheets.

Flowrate/sheet ml/h	Number of sheets	Flowrate total, ml/h	Cumulative % area	Cumulative % flowrate
<0.1	266	0	100.0	100.0
0.1-<0.2	13	1.3	29.1	100.0
0.2-<0.4	7	1.6	25.6	99.8
0.4-<0.8	10	5.6	23.7	99.6
0.8-<1.6	20	22.6	21.1	98.7
1.6-<3.2	19	46.1	15.7	95.2
3.2-<6.4	14	63.0	10.7	88.1
6.4-<12.8	12	108.5	6.9	78.4
12.8-<25.6	7	124.0	3.7	61.6
25.6-<51.2	6	215.0	1.9	42.5
>=51.2	1	60.0	0.3	9.3
Total	375	647.7		

2.4 CONCEPTUAL MODEL OF FLOW IN THE CHANNELS

The observations above indicate that most of the water flow takes place in a limited number of channels. The channels are seldom wider than a few meters and are often much narrower. If the observations reflect the flow paths in the bulk of the rock, there is considerably less sorption surface than if all the fractures are accessible to water flow. The visible fractures in granites and gneisses in Sweden have been found to be at spacings varying between tens of centimeters to a few meters. This would mean that the fracture trace length per m^2 of rock surface is typically in the range of 0.5 to 5 m/m^2. In the observations discussed above, 90 % of the flowrate takes place in one channel every 20 m^2 in Stripa, one channel every 85 m^2 in SFR, and 1 channel every 163 m^2 in the Kymmen tunnel. Assuming that a channel on the average is 1 m wide, it thus gives values of wet fracture length per area of 1/163 to 1/20 m/m^2. These figures may also be interpreted as average wet fracture spacings of 20 and 163 m if all fractures were parallel and of infinite extent. This means that there are some orders of magnitude less fracture surface to sorb on than if all the fractures were open.

It is not known how far the channels extend before meeting other channels. It seems reasonable to assume that the channels will not meet for at least a distance equal to the average distance between channels. This is in the order of the square root of the area per channel, so for 150 m^2 the distance is 12 m. The distance between intersections is probably much larger because if the channels are like thin widely spaced ribbons they are unlikely to intersect even for very long distances.

If the channels do not intersect for a certain distance then they may be modeled as a bundle of independent channels each with its own flowrate and wetted surface. Those channels with a large flowrate and small sorption surface will carry the tracers rapidly and in large amounts, thus dominating the nuclide transport.

If the water in the channels mixes regularly, then a mass of nuclides entering one channel will statistically move through all types of channels and the Advection-Dispersion case would apply.

3 CONCEPTS, MECHANISMS, AND MODELS FOR FLOW AND TRANSPORT IN FRACTURED ROCK

3.1 ADVECTION-DISPERSION MODEL

One of the simplest transport models is based on the assumption that the dissolved species are carried by the water with the average velocity of the water and that the variations of the species transport around the average velocity is a random process similar to molecular diffusion.

The concentration of a species in the water is then described by

$$\frac{\partial c}{\partial t} + u\frac{\partial c}{\partial z} = D_L \frac{\partial^2 c}{\partial z^2} \qquad (3.1)$$

where c = concentration in the liquid, mol/m^3
t = time, s
z = distance in direction of flow, m
u = water velocity, m/s
D_L = dispersion coefficient, m^2/s.

Equation (3.1) can be used to calculate how a radionuclide which does not interact with the solid material will move with the water. Decay is not accounted for in Equation (3.1) but is easily added when needed.

3.1.1 Sorption on surfaces

When the dissolved species sorb on the surfaces of the solid material it will be retarded in relation to the water velocity. For a linear instantaneous equilibrium Equation (3.1) is modified to become

$$R_a\frac{\partial c}{\partial t} + u\frac{\partial c}{\partial z} = D_L\frac{\partial^2 c}{\partial z^2} \qquad (3.2)$$

where R_a = surface retardation factor.

The retardation factor due to surface sorption is defined as

$$R_a = 1 + K_a a \tag{3.3}$$

where K_a = surface sorption coefficient, m

a = surface to volume ratio = $2/\delta$, m^2/m^3

δ = fracture aperture, m.

If the water velocity is u the nuclide velocity will be

$$u_N = \frac{u}{R_a} = \frac{u}{(1 + K_a \cdot a)} \tag{3.4}$$

For a given rock with a known flowrate per m^2 (Darcy velocity, u_o) the velocity "u" in the fractures is inversely proportional to the fracture aperture, assuming that the number of fractures is constant

$$u = u_o \cdot S / \delta \tag{3.5}$$

where S = average fracture spacing, m.

Inserting Equation (3.5) into (3.4) gives

$$u_N = \frac{u_o S}{\delta(1 + K_a \frac{2}{\delta})}$$

$$u_N = \frac{u_o S}{2 K_a} = \frac{u_o}{K_a a'} \quad \text{for } \frac{2 K_a}{\delta} >> 1 \tag{3.6}$$

where a' = wetted fracture area per volume of rock
$=2/S$, m^2/m^3.

For the sorbing nuclides the term $2K_a/\delta$ usually is >> 1, therefore the nuclide velocity is independent of the water velocity in the rock for a given flux (Darcy velocity). The nuclide velocity is then primarily determined by the flux, surface sorption coefficient, and by the wetted fracture surface in the rock.

It may be noted that the flow porosity of the rock does not influence the velocity of sorbing nuclides for a given Darcy velocity and fracture spacing under these circumstances.

The flux may be assessed as discussed above, K_a is determined by laboratory measurements but a', the wetted surface, must be assessed by field observations on actually flowing fractures. However, this is usually not done.

3.1.2 Matrix diffusion

In the case of surface sorption it is assumed that only the fracture surface in contact with the flowing water is available for sorption. In practice it may be expected that the rock nearest to the fracture surface will be penetrated by the dissolved diffusing species. The penetration depth will increase with increasing contact time. The rock volume, which may be expected to be accessed by diffusion during contact times of hundreds or more years, may have a considerably larger retardation effect than surface sorption alone may allow. On the other hand, the penetration depths for strongly sorbing nuclides, such as plutonium and neptunium, are not expected to be more than a few tens of centimeters even for contact times of hundreds of thousands of years. Most of the rock matrix then will not be penetrated and will not help in retarding the nuclides. The amount of rock accessed will depend on the sorption and diffusion properties of the matrix and the nuclides and also on the size of the surface area in contact with the mobile water from which the nuclides may diffuse into the matrix. In this case it was shown by Neretnieks /1980/ that the amount of wetted surface per volume of rock is one of the primary variables whereas the flow porosity, in practice, will have a negligible influence on the nuclide velocity for most sorbing nuclides.

3.2 "BUNDLE OF CHANNELS" MODEL

The "channeling model" states in essence that if the channel characteristics are known as well as the frequency of channels which carry a certain flowrate, then the transport in every channel is calculated individually and the sum of the effluents is calculated by adding the effluent concentration of all channels. In this case where the channels have been grouped in flowrate ranges, the effluent concentration from every group is calculated and multiplied by the fraction of flowrate in the respective group

$$c = \sum f_i \; c_i \tag{3.7}$$

where f_i = fraction of flowrate in group i
c_i = effluent concentration from a channel in group i, mol/m^3.

The concentration of the effluent from a channel will depend on the retardation and possible decay of the nuclides traveling through the channel. The main retardation effect is due to sorption within the rock matrix. Hydrodynamic dispersion is neglected in this case because "dispersion" due to the flowrate distribution will be considerably larger than that due to hydrodynamic dispersion.

The effluent concentration from a single channel has been modeled /Neretnieks et al., 1982/. In this case there is also the added influence of the porous matrix. The nuclide will diffuse into the micropores of the matrix and sorb on the inner surfaces of the matrix. This is given by

$$\frac{\partial c_f}{\partial t} + u_f \frac{\partial c_f}{\partial z} = \frac{2 D_e}{\delta} \frac{\partial c_p}{\partial x}\Big|_{x=0} - \lambda c_p \qquad (3.8)$$

where c_f = concentration in fracture water, mol/m^3
u_f = water velocity in fracture, m/s
D_e = effective diffusion coefficient, m^2/s
c_p = concentration in pore liquid, mol/m^3
x = distance into rock from fracture, m
λ = decay constant, s^{-1}.

The diffusion in the rock matrix is given by

$$\frac{\partial c_p}{\partial t} = D_a \frac{\partial^2 c_p}{\partial x^2} - \lambda c_p \qquad (3.9)$$

where D_a = apparent diffusion coefficient, mol/m^3.

The initial condition states that initially there is no nuclide in the water in the fracture and also no nuclide in the pore waters of the rock matrix. The boundary conditions state that at time zero the nuclide concentration is suddenly raised to c_o at the inlet of the fracture. If the inlet concentration decreases by radioactive decay the solution to the above equations becomes

$$c = c_o e^{-\lambda t} \operatorname{erfc}\left(\frac{(D_e K_d \rho_p)^{1/2} t_w}{(t - t_w)^{1/2} \delta}\right) \quad (3.10)$$

where K_d = mass sorption coefficient, m^3/kg
ρ_p = rock matrix density, kg/m^3
t_w = water residence time, s
c_o = initial concentration, mol/m^3.

Introducing the water residence time calculated as t_w equal to the channel volume divided by the flowrate in the channel, Equation (3.10) becomes

$$c = c_o e^{-\lambda t} \operatorname{erfc}\left(\frac{(D_e K_d \rho_p)^{1/2} LW}{(t - t_w)^{1/2} Q}\right) \quad (3.11)$$

where L = channel length, m
W = channel width, m
Q = channel flowrate, m^3/s.

The wetted fracture surface is an important entity because it is the surface in contact with the flowing water through which the nuclides diffuse into and sorb in the rock matrix. For sorbing nuclides and for contact times longer than the water residence time, the water residence time has little influence. The most important entities to assess are:

Water flowrate in a channel	Q
Wetted surface of a channel	2LW
Diffusivity in the rock matrix	D_e
Sorption coefficient in the matrix	K_d.

3.3 FREQUENT MIXING MODEL

Rasmuson (1985) studied the dispersion caused by channeling and determined the minimum number of mixing times required to obtain an approximate Gaussian response. The minimum number is a function of the channel aperture distribution (or of the flowrate distribution). If the number of connections is large, then the channels loose their identity by mixing with other channels. The outlet concentration may then be calculated from the mean flowrate. Therefore, the entity that is important to determine is the ratio of wet surface to the water flowrate for all the channels. For short distances, about 100 m, it may be expected that the number of mixing

occasions is small, but for long distances a large number of mixings may be expected to occur. Then, the outlet concentration will be modified by the existence of mixing between the channels.

3.4 THE ADVECTION-DISPERSION-MATRIX DIFFUSION MODEL

In the "bundle of channels" model, we assumed that the dispersion in each channel is negligible if compared with the dispersion caused by channeling. The solution of the equations, using the numerical code TRUCHN, requires at least some dispersion in the channels to avoid numerical oscillations.

The model considers the transport of contaminants in a fluid which flows through a thin fracture. The dispersion is take into account by applying hydrodynamic dispersion in the fracture.

Assuming a linear sorption isotherm for the surface sorption and using the surface retardation factor R_a, the differential equation for the fracture becomes

$$\frac{\partial c_f}{\partial t} - \frac{D_L}{R_a}\frac{\partial^2 c_f}{\partial z^2} + \frac{u_f}{R_a}\frac{\partial c_f}{\partial z} - \frac{2}{\delta}\frac{D_e}{R_a}\frac{\partial c_p}{\partial x}\bigg|_{z=0} = 0 \qquad (3.12)$$

$$0 \le z \le \infty$$

Equation (3.9) is used to model the diffusion in the rock matrix.

3.5 CHAIN DECAY MODELING

Chain decay is modeled by having one equation each of Equations (3.8) and (3.9) for every nuclide and accounting for the production of the daughter nuclide by the parent /Rasmuson et al., 1982/.

4 DATA USED IN CALCULATIONS

4.1 CHANNEL STATISTICS AND PROPERTIES USED

Transport of nuclides from the WP-Cave repository is calculated for different migration distances, flowrates, and sorption coefficients. The channeling model is tested for different situations and then compared with the mixing model.

The calculation of nuclide migration by channeling requires that the geometrical characteristics of the channels are known. The flow distribution between the channels must also be known. Thus, it is assumed that the flowrate distribution observed on the ceiling of the four main tunnels at the SFR repository may be extended to the rock mass between the repository and the biosphere.

For calculation purposes the channels are divided into 6 groups with flowrate ranges increasing in a geometric progression. The number of channels and the fraction of the total flow in each channel group are needed for these calculations and are shown in Table 4-1. The flow in each channel is calculated from the fraction of flow and the number of channels in each group and the total flux in the rock. The flowrates per channel listed in Table 4-1 are for an average flowrate of 1.0 l/m^2a. The flowrate distribution values listed in Table 4-1 are taken directly from SFR. For the present calculations, the flowrates have been multiplied by a factor of 0.3 to correspond to an average flowrate of 0.3 l/m^2a.

Table 4-1 Fraction of the total flowrate which flows in the different groups of channels.

Flowrate range l/min**	Would be flowrate per channel $m^3/s \cdot 10^{-8}$*	Fraction of channels**	Fraction of flowrate**	Flowrate channel group
>=1.6	2.940	0.01	0.13	1
0.8-<1.6	1.653	0.02	0.15	2
0.4-<0.8	0.772	0.07	0.21	3
0.2-<0.4	0.333	0.26	0.30	4
0.1-<0.2	0.149	0.23	0.13	5
<0.1	0.056	0.4	0.08	6

* The hydraulic gradient is $4 \cdot 10^{-3}$ m/m and the hydraulic conductivity is $8 \cdot 10^{-9}$ m/s. These values give an average flowrate of 1.0 l/m^2a.

** Values taken from Table 2.1.

4.2 SORPTION AND DIFFUSION DATA

Table 4-2 shows half-lives and sorption coefficients for the radionuclides (fission products) used in the calculations. The sorption coefficients for each nuclide are for both the reduced and oxidized conditions with the exception of ^{99}Tc. For this nuclide it is listed separately for the reduced and oxidized sorption coefficients. The sorption coefficients are for granitic rock. The list of nuclides are obtained from Lindgren and Skagius /1989/.

Table 4-2 Half-lives and sorption coefficients for fission products.

Nuclides	Half-life years	Sorption coefficient $(K_d\rho_p)$ m^3/m^3
^{14}C	$5.7 \cdot 10^3$	0.01
^{59}Ni	$7.5 \cdot 10^4$	540
^{79}Se	$6.5 \cdot 10^4$	0.01
^{93}Zr	$1.5 \cdot 10^6$	10,800
^{94}Nb	$2.0 \cdot 10^4$	10,800
^{99}Tc (red)	$2.1 \cdot 10^5$	135
^{99}Tc (ox)	$2.1 \cdot 10^5$	0.54
^{107}Pd	$6.5 \cdot 10^6$	0.01
^{126}Sn	$1.0 \cdot 10^5$	0.01
^{129}I	$1.6 \cdot 10^7$	0.01
^{135}Cs	$3.0 \cdot 10^6$	135

In this report, we will also study four decay chains for the actinides. The actinides are, in general, substances with high sorption properties under reducing conditions. These conditions may be expected to occur in deep repositories. For the WP-Cave repository the effect of oxidizing conditions will also be investigated. The sorption coefficients of the different radionuclides are shown in Table 4-3.

Table 4-3 Sorption coefficients for actinides.

Nuclides	Sorption coefficient, m^3/kg Reducing conditions	Oxidizing conditions
Am	5	5
Pu	5	5
Np	5	0.1
U	5-(1)*	0.05
Pa	5	5
Th	5	5
Ra	0.1	0.1

* Value used in variation calculations.

The decay chains of the actinides in the spent fuel used in the calculations are listed in Table 4-4. The parent and daughter nuclides chosen for each chain are denoted by M and D1, D2, respectively /Lindgren and Skagius, 1989/.

4.3 REFERENCE DATA

The following data have been used in the calculations:

Water flowrate in rock	u_o = 0.3 l/m^{2}a
Fracture width	W = 1 m
Fracture length	L = 100 m
Fracture aperture	δ = 0.25 mm
Density of rock matrix	ρ_p = 2700 kg/m^3
Rock effective diffusivity	D_e = 5·10^{-14} m^2/s
Peclet number	Pe = 10
Flowrate distribution	SFR.

The flowrate distribution found in the SFR site will be used in these calculations. The implications of using other flowrate distribution will be discussed later.

Table 4-4 Actinide decay chains.

	Nuclide	Half-life*
Chain 1 (4N+1)	^{237}Np (M)	$2.10 \cdot 10^{6}$ Y
	^{233}Pa	27 D
	^{233}U (D1)	$1.60 \cdot 10^{5}$ Y
	^{229}Th (D2)	7340 Y
	^{225}Ra	14.8 D
Chain 2 (4N+3)	^{239}Pu (M)	$2.40 \cdot 10^{4}$ y
	^{235}U (D1)	$2.00 \cdot 10^{8}$ Y
	^{231}Th	25.5 H
	^{231}Pa (D2)	$3.20 \cdot 10^{4}$ Y
	^{227}Ac	21.8 Y
	^{227}Th	18.2 D
Chain 3 (4N)	^{240}Pu (M)	6537 Y
	^{236}U (D1)	$2.30 \cdot 10^{7}$ Y
	^{232}Th (D2)	$1.40 \cdot 10^{10}$ Y
	^{228}Ra	5.75 Y
	^{228}Ac	6.13 H
	^{228}Th	1.9 Y
Chain 4 (4N+2)	^{242}Pu	$3.80 \cdot 10^{5}$ Y
	^{238}U (M)	$4.50 \cdot 10^{9}$ Y
	^{234}Th (D1)	24.1 D
	^{234}U	$2.50 \cdot 10^{5}$ Y
	^{230}Th (D2)	$7.70 \cdot 10^{4}$ Y
	^{226}Ra (D3)	1602 Y

* (Y = years, D = days, H = hours.)

5 CALCULATED RESULTS FOR CHANNELING AND MIXING MODELS

5.1 SAMPLE CALCULATIONS FOR ^{94}Nb, ^{99}Tc, and ^{129}I

To illustrate the influence on the effluent concentration from the different channels, breakthrough curves for ^{94}Nb, ^{99}Tc (reducing conditions), and ^{129}I at a distance of 100 m and for a flux of 0.3 l/m^2a are calculated. The inlet concentration, c_o, for each nuclide is set equal to 1.0 at time zero. It decays with the half-life. The outlet concentration for each group of channels and the effluent concentration for all the channels are shown in Figures 5-1 - 5-3. The results show that for strongly sorbing nuclides (^{99}Tc, ^{94}Nb) the channels in group 1 allow little decay. Channels in group 2 carry about half as much water per channel as those in group 1 and allow some more decay. Channels in group 6 are the channels which carry the least water per channel and there the nuclides have considerable decay. For the nonsorbing or weakly sorbing nuclides the channel's flowrate has very little effect on the decay of the nuclides. The total effluent concentration from all the channels is obtained by a weighted concentration of the effluent from each of the channels (Equation (3.7)). The calculations are based on a flux of 0.3 l/m^2a, travel distance of 100 m, fracture width of 1 m, and an aperture size of 0.25 mm.

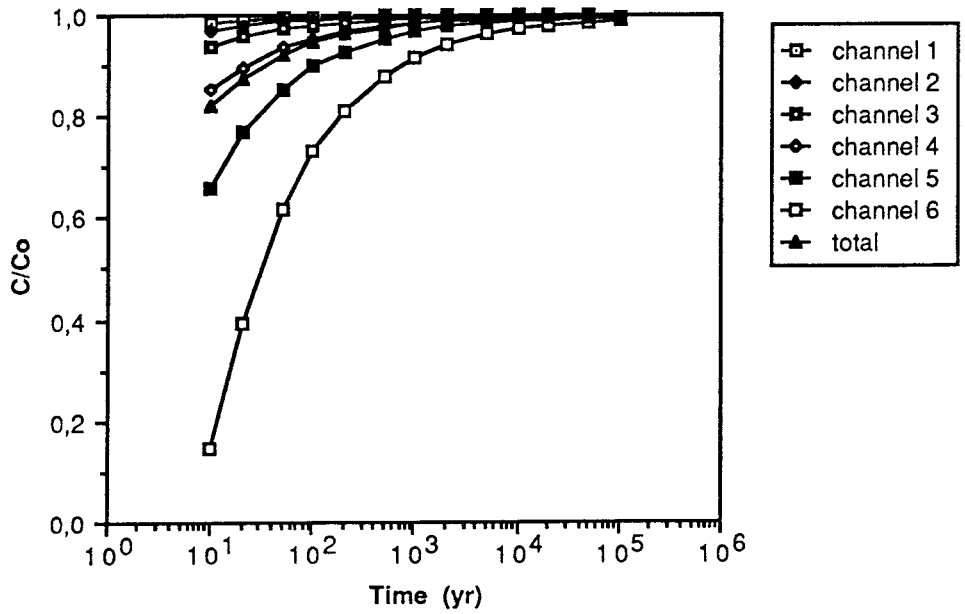

Figure 5-1 Effluent concentration in the different groups of channels for ^{129}I where channel 1 has the largest flowrate and channel 6 has the smallest flowrate.

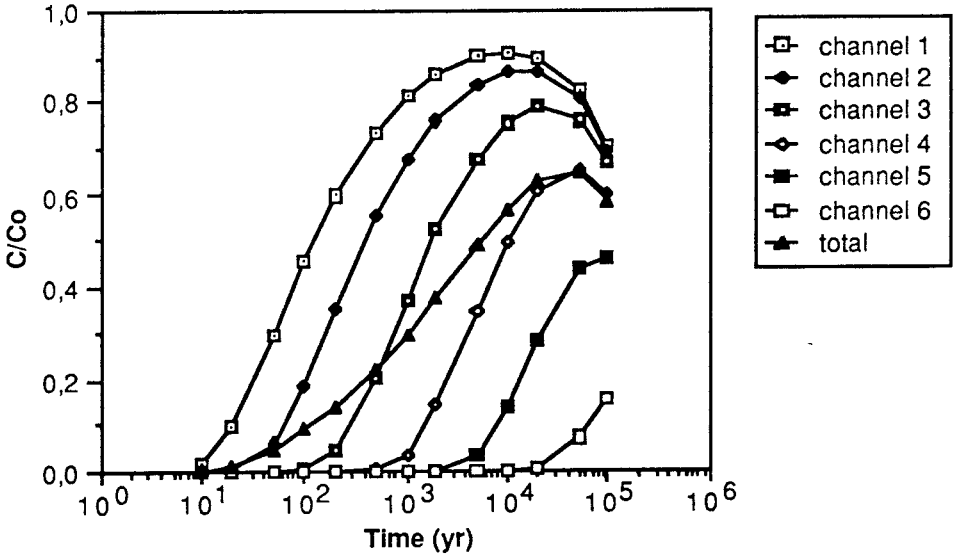

Figure 5-2 Effluent concentration in the different groups of channels for ^{99}Tc (reducing conditions) where channel 1 has the largest flowrate and channel 6 has the smallest flowrate.

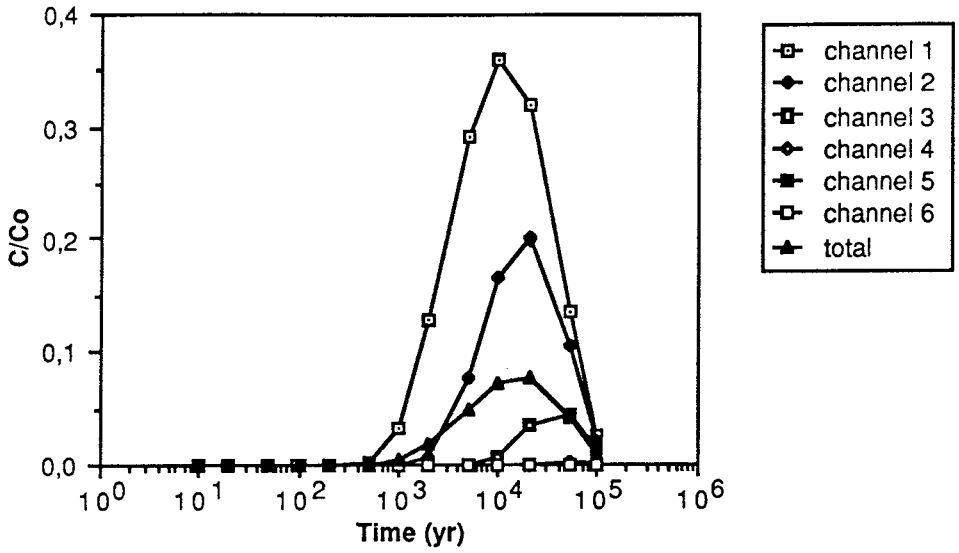

Figure 5-3 Effluent concentration in the different groups of channels for ^{94}Nb where channel 1 has the largest flowrate and channel 6 has the smallest flowrate.

5.2 CHANNEL APERTURE INFLUENCE ON OUTLET CONCENTRATION

For the larger times the channel aperture has little or no impact, but for very short times it has a slight impact. In the base case example a channel aperture of δ = 0.25 mm is used. Calculations are also made for other aperture sizes and the results are shown in Figure 5-4. The calculations for ^{129}I, ^{99}Tc, and ^{94}Nb are for a migration distance of 100 m and two different channel apertures, 0.1 mm and 1.0 mm. For ^{129}I the results are identical for times larger than about 20 years, so the channel aperture influences only those results for times less than a few years. The results also conclude that the aperture change has no real effect on the nuclides ^{94}Nb and ^{99}Tc at any time. It is expected that there will be no difference between the small and large channels for any sorbing nuclides for times longer than a few tens of years.

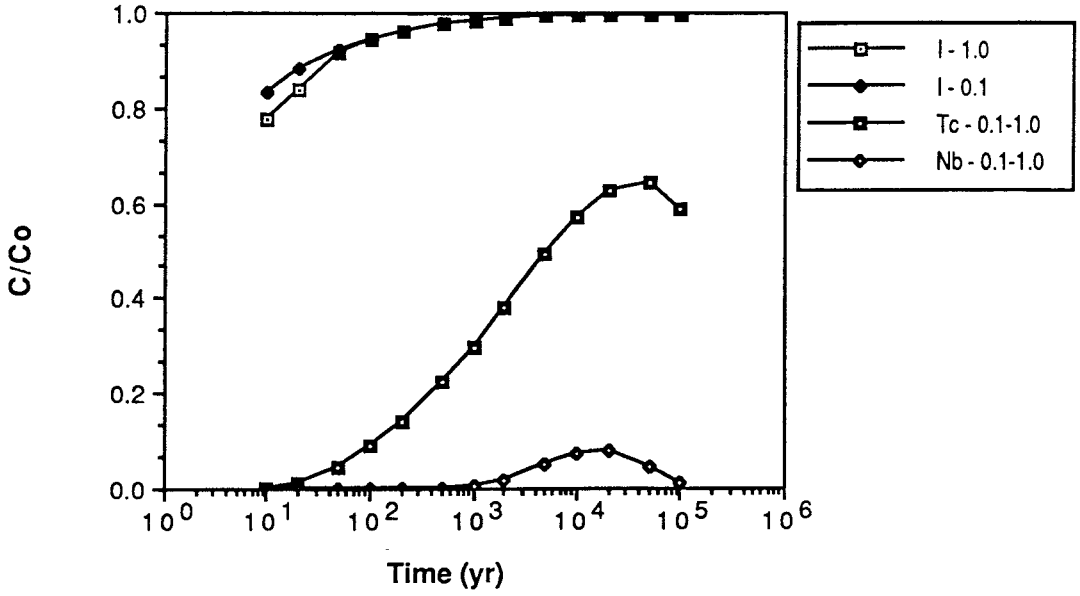

Figure 5-4 Plot of relative concentrations for different aperture sizes, 0.1 mm and 1.0 mm, for ^{94}Nb, ^{99}Tc, and ^{129}I.

5.3 CHANNELING MODEL WITH DISPERSION

In the calculations above, it is assumed that the dispersion in each channel is negligible if compared to the dispersion caused by channeling. Figure 5-5 shows the influence on the concentration at the outlet if a given dispersion is considered in the channels. A value of 10 is assumed for the Peclet number. This value is base on compiled results by Neretnieks /1985/ from different laboratory tests and in situ tracer tests. Neretnieks found that the dispersion increases with distance and a value of 10 for the Peclet number was determined from these data. The other values used are the same as the base case values.

The results show a slight increase of the concentration at the outlet when dispersion in the channels is considered. An increase in the concentration is noticed for ^{94}Nb and ^{99}Tc at shorter times. No change is observed for ^{129}I. Since the calculations that include dispersion require more computing effort, the solutions without dispersion are sufficient for the accuracy required in these calculations.

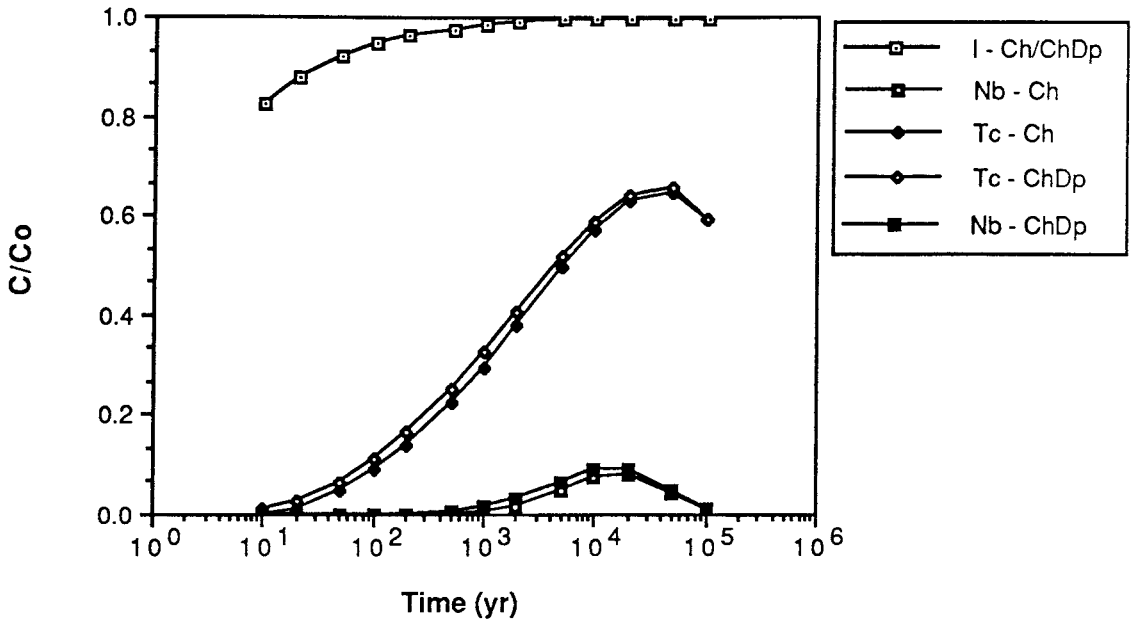

Figure 5-5 Plot of relative concentrations as a function of dispersion in the channels (ChDp) in comparison to the case with no dispersion in the channels (Ch) for ^{94}Nb, ^{99}Tc, and ^{129}I.

5.4 IMPACT OF CHANGES IN MODEL PARAMETERS

In the calculations above, a base case is chosen. The channel width is assumed to be 1 meter wide and the channel aperture 0.25 mm. It is also assumed that the dispersion in each channel is negligible if compared with the dispersion caused by the channeling.

The concentration at the outlet at a given time is determined by the value of the group

$$\frac{L\,W\,(D_e\,K)^{1/2}}{Q}$$

It can be seen that a decrease of the channel width W by a factor of 2 may be compensated by an increase in the channel length L by the same factor. The influence of the channel flowrate Q is also seen. If the width of the channel is reduced to 0.50 m and the effluent concentration at 200 m is required, the values calculated above may be used. Similar results may be obtained for other values of the flux or sorption coefficient.

To illustrate the effects of varying these parameters by a factor of 2, calculations were performed for ^{94}Nb, ^{99}Tc, and ^{129}I. Letting the above expression be denoted by the symbol F, calculations were done for F varying between 4F (the best case) and F/8 (the worst case). The base case, F, concentrations are calculated with a flux of 0.3 l/m^2a, fracture width of 1 m, and travel distance of 100 m. Intermediate cases for the concentrations are determined by which the travel distance, fracture width, and flux are altered from the base case values. The case 4F represents, for example, the nuclide traveling a distance of 200 m at either a flowrate of 0.15 l/m^2a or through a fracture width of 2.0 m. The F/8 case would represent just the opposite situation. It consists, for example, of the nuclides traveling a distance of 50 m at a flux of 0.6 l/m^2a in a fracture with a width 0.5 m. Results for the 6 cases for the 3 nuclides are shown in Figures 5-6 - 5-8. Maximum relative concentrations for various situations for the 3 nuclides are listed in Table 5-2. The nonsorbing nuclide ^{129}I shows practically no change from the 4F to the F/8 case while the high sorbing nuclide ^{94}Nb shows considerable change.

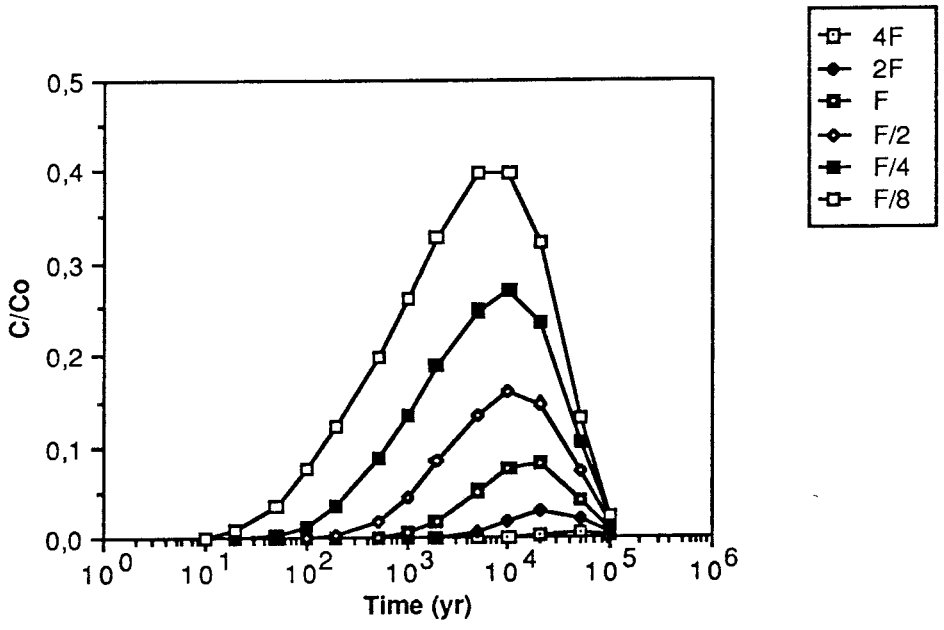

Figure 5-6 Relative concentrations for ^{94}Nb influenced by the effect of varying the channel parameters L, W, and Q, where $F = LW(D_eK)^{1/2}/Q$.

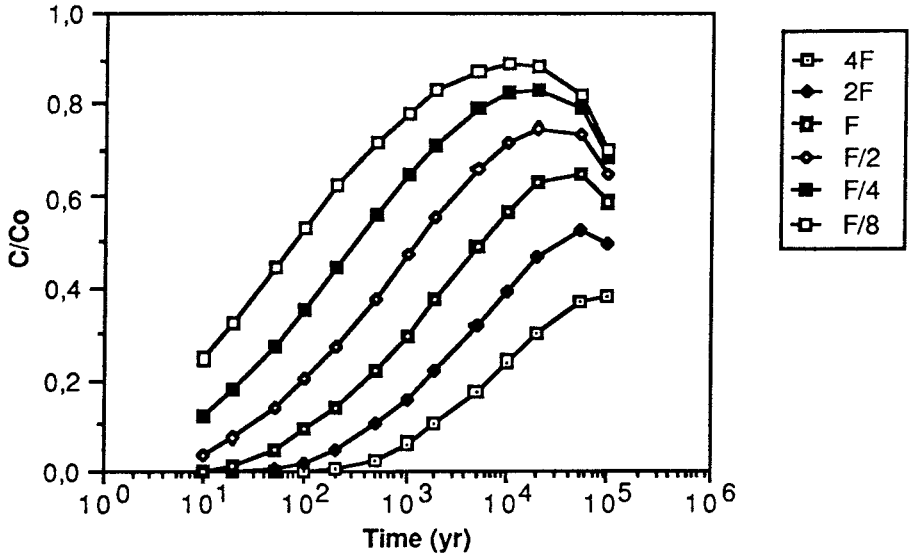

Figure 5-7 Relative concentrations for ^{99}Tc influenced by the effect of varying the channel parameters L, W, and Q, where $F = LW(D_eK)^{1/2}/Q$.

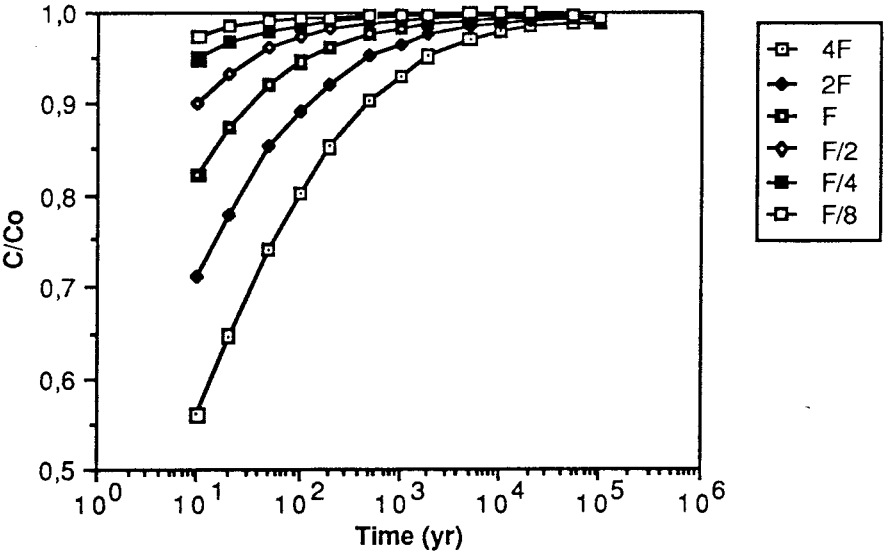

Figure 5-8 Relative concentrations for ^{129}I influenced by the effect of varying the channel parameters L, W, and Q, where $F = LW(D_eK)^{1/2}/Q$.

Table 5-2 Maximum relative concentration for the different radionuclides from the effect of varying the channel parameters L, W, and Q.

VARIATION OF CHANNEL PARAMETER CASES, $F = LW(D_eK)^{1/2}/Q$						
Nuclides	F/8	F/4	F/2	F	2F	4F
^{94}Nb	.3981	.2690	.1576	.0794	.0299	.0064
^{99}Tc	.8921	.8346	.7495	.6451	.5241	.3724
^{129}I	.9989	.9982	.9972	.9954	.9922	.9888

5.5 CALCULATIONS WITH MIXING MODEL

The channeling model assumes that channels do not intersect each other from the repository to the nearest fracture zone. As it is discussed above, for long distances it is expected that the channels intersect to some extent along their paths. If the channels intersect many times, the identity of the channels is lost. In this case the transport of radionuclides is determined by the ratio of the total wet surface to the water flux. The results are presented in Figure 5-9. The mixing model outlet concentration is much less than the outlet concentration when channels with different water flowrates are used. An average flowrate is used in the mixing model which falls between the flowrates in channel groups 4 and 5 in Figures 5-1 to 5-3. Therefore, the outlet concentrations for the mixing model can be obtained by interpolating between the groups 4 and 5.

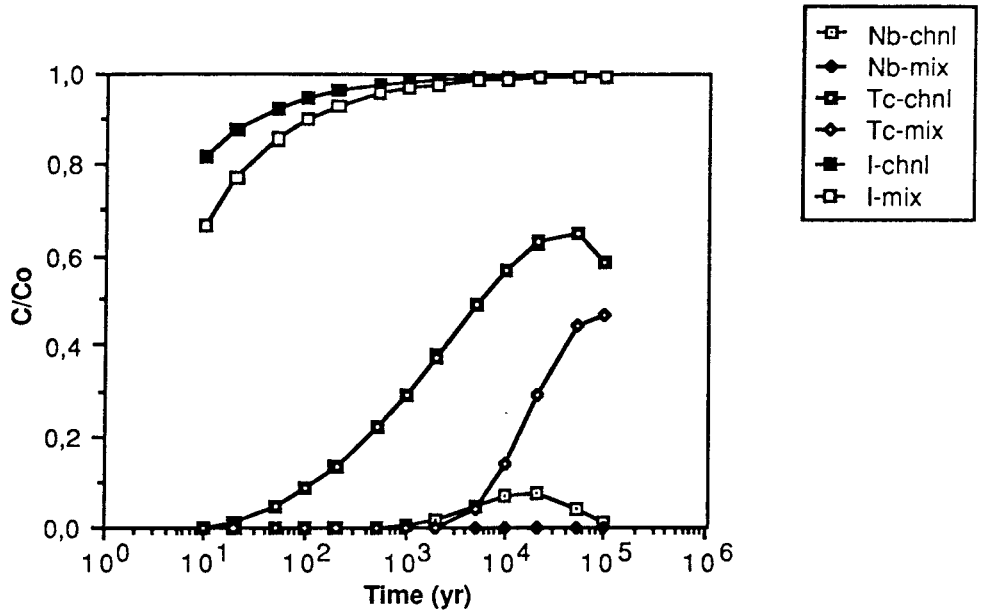

Figure 5-9 Relative concentrations for different radionuclides for flow in channels with the same flowrate (mixing model) in comparison to flow in channels with different flowrates (channeling model).

6 FAR-FIELD RELEASE RATE OF FISSION PRODUCTS

6.1 MAXIMUM RELEASE RATES OF ESCAPING NUCLIDES

Calculations using the channeling model with base case parameter values were performed to determine the maximum release for ten fission product nuclides escaping from the WP-Cave sand-bentonite barrier to the biosphere. The hydraulic cage surrounding the repository has been omitted for these calculations. The input release rate curves for each nuclide was supplied by Skagius et al. /1988/. They assumed that the concentration around the canister is determined by the rate of dissolution of the uranium-dioxide matrix of the fuel. For the rate assumed the total time for this dissolution is about 20,000 years The output release rate curves are calculated for both no decay and decay cases. The release rate curve for each nuclide is the total sum of the effluent release from each channel group multiplied by the fraction of the flowrate in that group. The release rate curves from the far-field (geosphere) to the biosphere for the radionuclides ^{94}Nb, ^{126}Sn, and ^{129}I are presented in Figures 6-1 - 6-3. The time axis in the figures is the time after canister breakthrough. In Figure 6-4, a summary of the release rate curves, which include decay, for the ten nuclides is presented and the maximum release rates for the decay and no decay cases for each nuclide are listed in Table 6-1.

The nonsolubility limited nuclides, ^{94}Nb and ^{129}I, represent the conditions of high sorption, short half-life and no sorption, long half-life, respectively. These nuclides are shown in Figures 6-1 and 6-3. Comparing the near-field and far-field releases without decay in Table 6-1 for these two nuclides, we found very little change (if any) between the maximum release rates. For the near-field and far-field release rates with decay, hardly any change is noticed for ^{129}I but for ^{94}Nb the release rate is decreased by a factor of about 10. This difference is due to the nuclide's high sorption characteristic and relatively short half-life. In the case for ^{129}I, the negligible change in the rate is due to the nuclide having no sorption and a long half-life. The five remaining nonsolubility limited nuclides follow the same trend established by these two nuclides (e.g., ^{93}Zr decay release rate is decreased by a factor of about 2 due to its high sorption capability and long half-life). Figures illustrating the release rate of the

remaining nonsolubility limited nuclides are found in Appendix A, Figures A-1 to A-4 and A-7.

The solubility limited nuclide ^{126}Sn is presented in Figure 6-2 for the far-field decay case only. The maximum release rate of $0.96.10^{-1}$ GBq/a for ^{126}Sn is limited by its solubility. This constant level is reached due to it having no sorption and a rather long half-life. The nuclide ^{107}Pd follows the same trend in reaching a maximum constant release determined by its solubility limit. However, for ^{99}Tc the maximum release rate never is constant due to its intermediate sorption capability. These results are presented in Table 6-1 and the release rate curves for ^{99}Tc and ^{107}Pd are found in Appendix A, Figures A-5 and A-6.

From these calculations for the ten fission product nuclides, the transport of the radionuclides is seen to be retarded very little (if any) through the surrounding rock at a transport distance of 100 meters and fracture width of 1 meter. Only the high sorbing and/or short half-life nuclides exhibit any decrease in the release rate in the surrounding rock.

The dose rates in Sv/a for all the radionuclides are listed in Table 6-2. The conversion factors for activity released to the biosphere to dose for each nuclide are supplied by Bergström and Nordlinder /1987/. The cases presented are for the well, lake, and a mixed case consisting of the well and lake cases. The calculated dose rates for all the nuclides are within the exposure limit of 10^{-4} Sv/a.

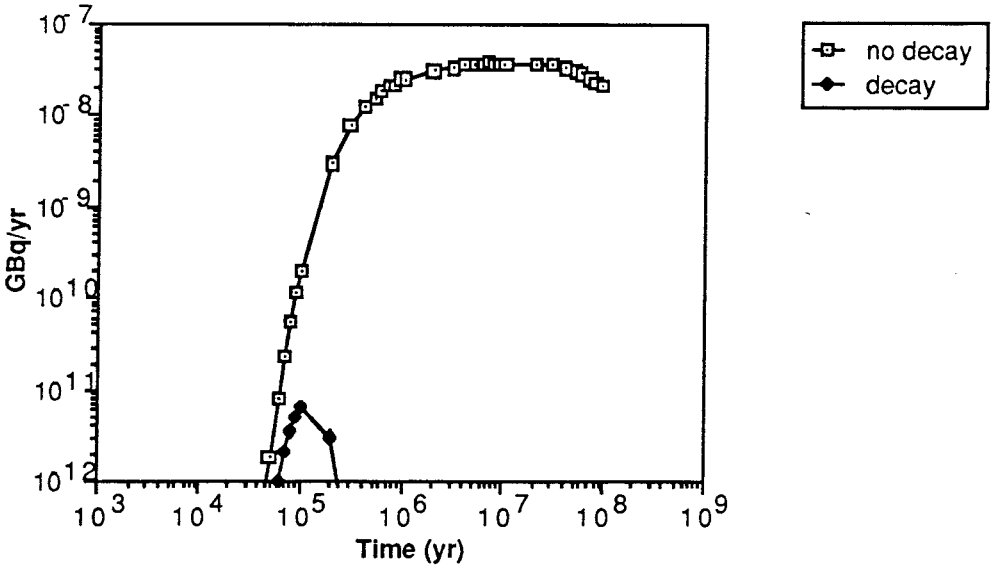

Figure 6-1 Release rates of ^{94}Nb from the far-field to the biosphere.

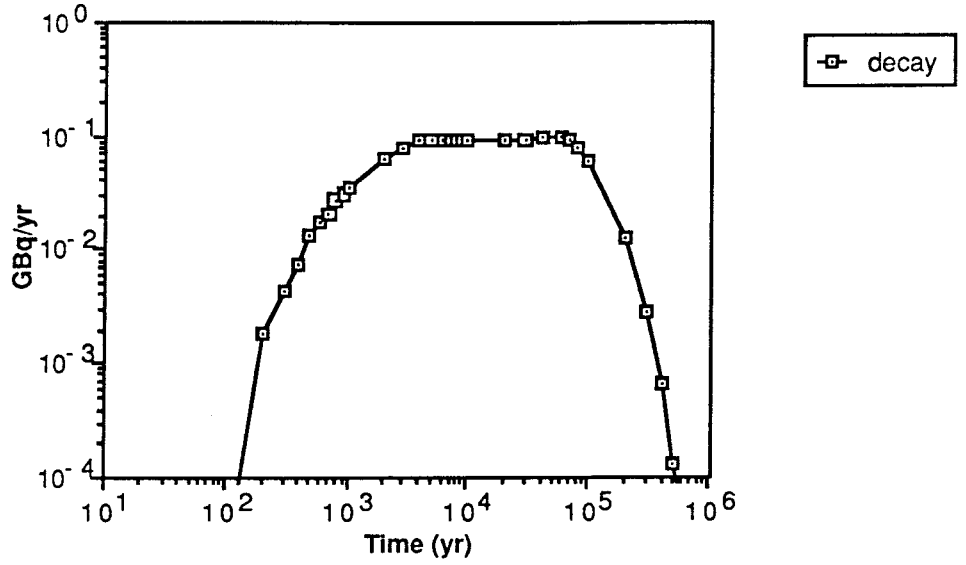

Figure 6-2 Release rate of ^{126}Sn from the far-field to the biosphere.

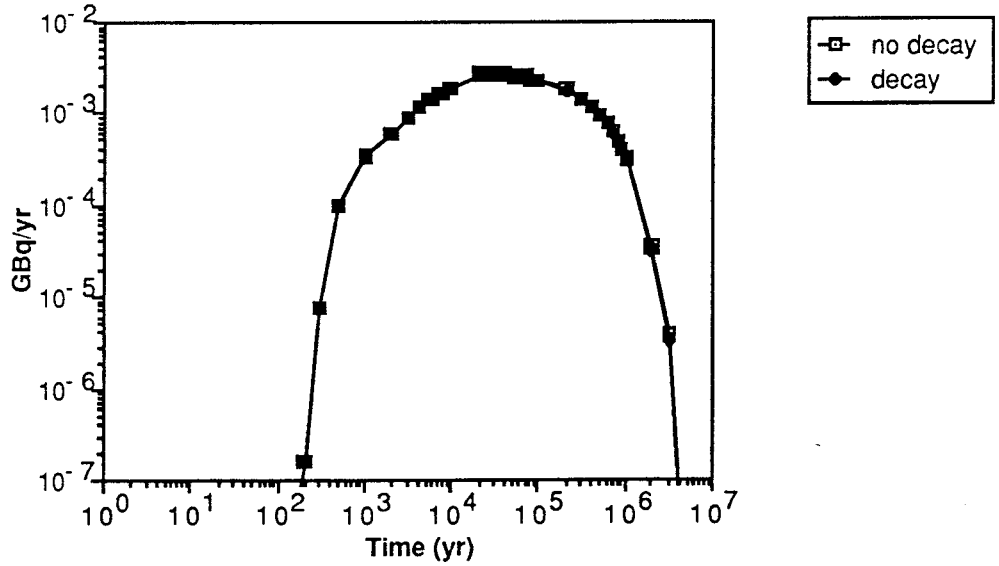

Figure 6-3 Release rates of ^{129}I from the far-field to the biosphere.

Table 6-1 Maximum concentration rates for the radionuclides.

	MAXIMUM RELEASE RATE (GBq/a)			
	FROM NEAR-FIELD		FROM FAR-FIELD	
NUCLIDE	NO DECAY	DECAY	NO DECAY	DECAY
^{14}C	$1.6 \cdot 10^{-1}$ 21,000 yrs	$4.7 \cdot 10^{-2}$ 4,500 yrs	$1.6 \cdot 10^{-1}$ 21,000 yrs	$4.6 \cdot 10^{-2}$ 4,500 yrs
^{59}Ni	$5.8 \cdot 10^{-3}$ 250,000 yrs	$2.0 \cdot 10^{-3}$ 80,000 yrs	$5.2 \cdot 10^{-3}$ 3,000,000 yrs	$1.1 \cdot 10^{-3}$ 100,000 yrs
^{79}Se	$3.4 \cdot 10^{-2}$ 23,000 yrs	$2.7 \cdot 10^{-2}$ 21,000 yrs	$3.4 \cdot 10^{-2}$ 23,000 yrs	$2.7 \cdot 10^{-2}$ 21,000 yrs
^{93}Zr	$1.6 \cdot 10^{-4}$ 4,400,000 yrs	$6.1 \cdot 10^{-5}$ 1,500,000 yrs	$1.4 \cdot 10^{-4}$ 30,000,000 yrs	$3.4 \cdot 10^{-5}$ 2,000,000 yrs
^{94}Nb	$4.6 \cdot 10^{-8}$ 3,200,000 yrs	$5.2 \cdot 10^{-11}$ 110,000 yrs	$3.7 \cdot 10^{-8}$ 7,000,000 yrs	$7.6 \cdot 10^{-12}$ 120,000 yrs
^{99}Tc		$1.1 \cdot 10^{-4}$* 600 yrs		$9.2 \cdot 10^{-5}$ 500,000 yrs
^{107}Pd		$3.5 \cdot 10^{-7}$* 50 yrs		$3.5 \cdot 10^{-7}$ 1000 yrs
^{126}Sn		$9.6 \cdot 10^{-2}$* 4000 yrs		$9.6 \cdot 10^{-2}$ 5000 yrs
^{129}I	$2.7 \cdot 10^{-3}$ 22,000 yrs	$2.7 \cdot 10^{-3}$ 22,000 yrs	$2.7 \cdot 10^{-3}$ 22,000 yrs	$2.7 \cdot 10^{-3}$ 22,000 yrs
^{135}Cs	$4.2 \cdot 10^{-4}$ 130,000 yrs	$4.1 \cdot 10^{-4}$ 120,000 yrs	$3.8 \cdot 10^{-4}$ 900,000 yrs	$3.4 \cdot 10^{-4}$ 300,000 yrs

* Nuclide release is limited by the solubility.

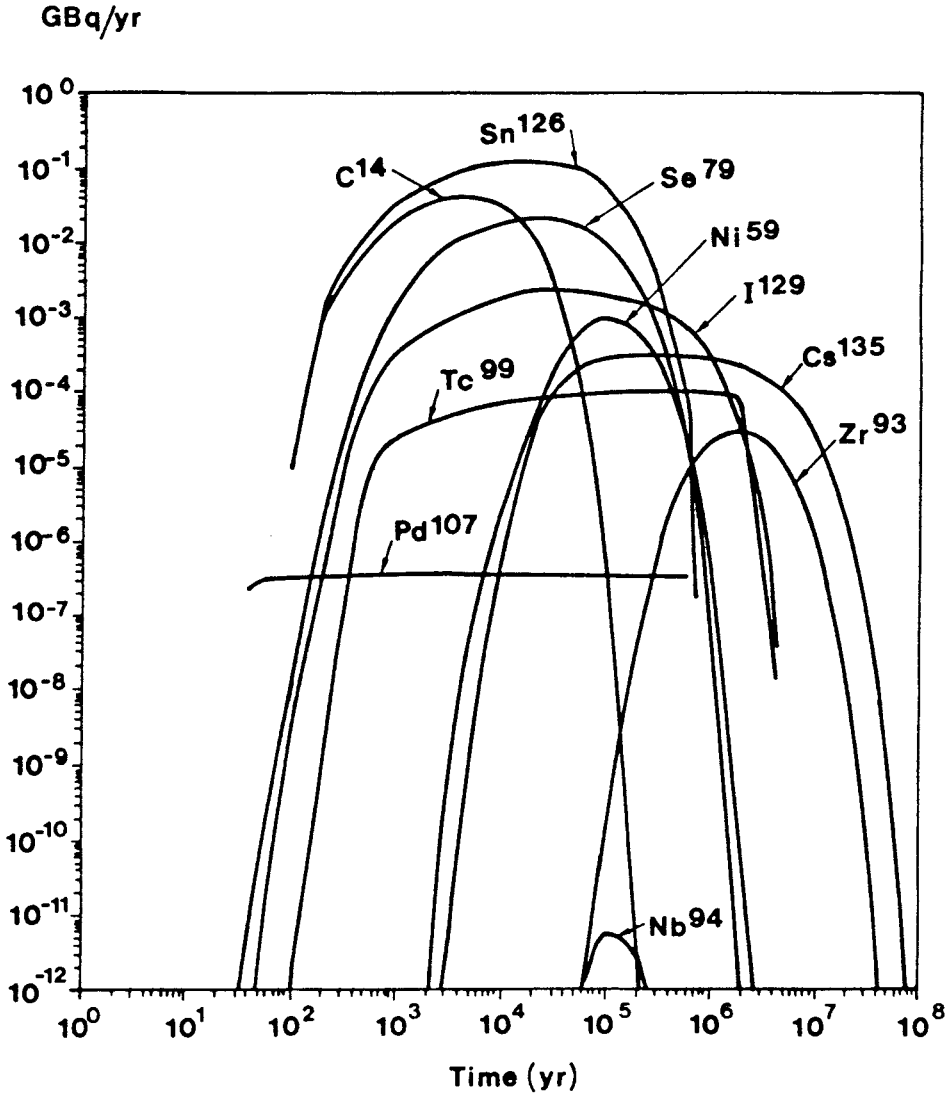

Figure 6-4 Plot of release rates to the biosphere for the ten studied radionuclides. Release rates from the repository have been supplied by Skagius et al. /1988/.

Table 6-2 Maximum dose rates of the studied radionuclide escaping from the repository to the biosphere**.

RADIONUCLIDE	MIXED* Sv/a	WELL Sv/a	LAKE Sv/a
^{14}C	$4.0 \cdot 10^{-6}$	$2.3 \cdot 10^{-8}$	$4.0 \cdot 10^{-6}$
^{59}Ni	$1.1 \cdot 10^{-10}$	$7.3 \cdot 10^{-11}$	$4.8 \cdot 10^{-11}$
^{79}Se	$1.5 \cdot 10^{-6}$	$1.8 \cdot 10^{-7}$	$1.3 \cdot 10^{-6}$
^{93}Zr	$8.1 \cdot 10^{-11}$	$8.1 \cdot 10^{-11}$	$3.7 \cdot 10^{-11}$
^{94}Nb	$7.5 \cdot 10^{-17}$	$1.4 \cdot 10^{-15}$	$5.1 \cdot 10^{-17}$
^{99}Tc	$4.4 \cdot 10^{-11}$	$2.9 \cdot 10^{-11}$	$3.0 \cdot 10^{-11}$
^{107}Pd	$2.4 \cdot 10^{-16}$	$1.5 \cdot 10^{-16}$	$1.0 \cdot 10^{-16}$
^{126}Sn	$2.9 \cdot 10^{-6}$	$5.8 \cdot 10^{-7}$	$2.4 \cdot 10^{-6}$
^{129}I	$1.3 \cdot 10^{-6}$	$7.3 \cdot 10^{-7}$	$9.0 \cdot 10^{-7}$
^{135}Cs	$4.5 \cdot 10^{-8}$	$1.1 \cdot 10^{-9}$	$4.1 \cdot 10^{-8}$

* The mixed case is a combination of the well and lake cases.
** Biosphere conversion dose rates have been supplied by Bergström and Nordlinder /1987/.

6.2 INFLUENCE OF AN INCREASE OF FLOWRATE

The water flowrate was increased by a factor of 10 to 3.0 l/m^2yr to determine its effect on the maximum release rate of the radionuclides. Three nuclides were selected. These nuclides are ^{94}Nb, ^{126}Sn, and ^{129}I. The conclusion drawn from the flowrate increase is that the maximum release rate of the nuclides is considerably increased. For ^{129}I and ^{126}Sn the increase was about a factor 3. ^{94}Nb increased by about a factor 20. The increased release from the near-field accounts for a factor of 3 and the rest is due to a smaller decay in the far-field.

7 FAR-FIELD RELEASE RATE OF ACTINIDES AND DAUGHTER NUCLIDES.

The release rates from the sand-bentonite barrier are the input to the contaminant transport in the fractures in the rock. These values were calculated by Lindgren and Skagius /1988/. For the rate of dissolution of the uranium-dioxide used in these calculations the total time for this dissolution is about 1,200,000 years. The release rates of the fission products were calculated assuming a dissolution time of 20,000 years.

Preliminary tests were performed to determine an adequate grid to be used in this kind of problem. More details are shown in Appendix B.

In the next section, we calculate the release from the geosphere into the biosphere, the so called far-field release. The implications of the use of other values for water flowrates, transport lengths, and sorption properties will be discussed in Section 7.3.

7.1 RELEASE TO THE BIOSPHERE

The calculations performed include the release to the biosphere of ^{242}Pu and of the four chains shown in Table 4-4.

7.1.1 Release of radionuclide ^{242}Pu

Figure 7-1 shows the release to the biosphere for radionuclide ^{242}Pu. The release from the sand-bentonite barrier is also shown. The maximum release from the sand-bentonite barrier is $2.0 \cdot 10^{-4}$ GBq/a and will occur at time $6.0 \cdot 10^{5}$ years. The maximum release to the biosphere is $0.85 \cdot 10^{-4}$ GBq/a and will occur at time $7.0 \cdot 10^{5}$ years. This means that the maximum release of ^{242}Pu is reduced to about 40 % of the input value.

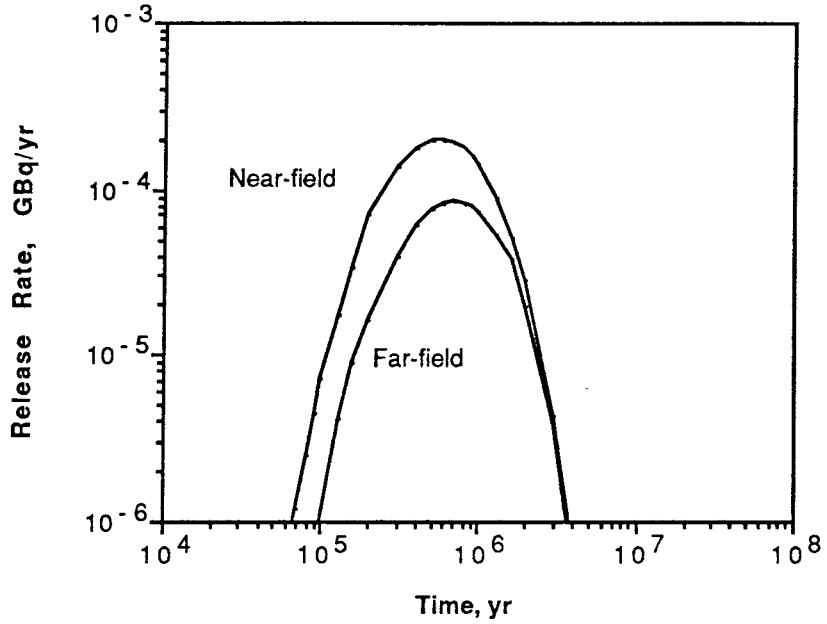

Figure 7-1 Release from the far-field for radionuclide ^{242}Pu. Release from the near-field (sand-bentonite barrier) is also shown.

7.1.2 Release of the radionuclides in Chain 1 (4N+1)

The nuclides in Chain 4N+1 studied in this report are shown in Table 4-4. ^{237}Np is the parent radionuclide for this chain, and ^{233}U and ^{229}Th are the daughter radionuclides. Figure 7-2 shows the release from the sand-bentonite barrier. The resulting releases from the far-field are shown in Figure 7-3.

The release for ^{237}Np and ^{233}U are reduced to about 50 % by the far-field. For ^{229}Th the situation is different. The release of ^{229}Th is determined by the decay of ^{233}U. The contribution from ^{229}Th released from the sand-bentonite barrier is insignificant.

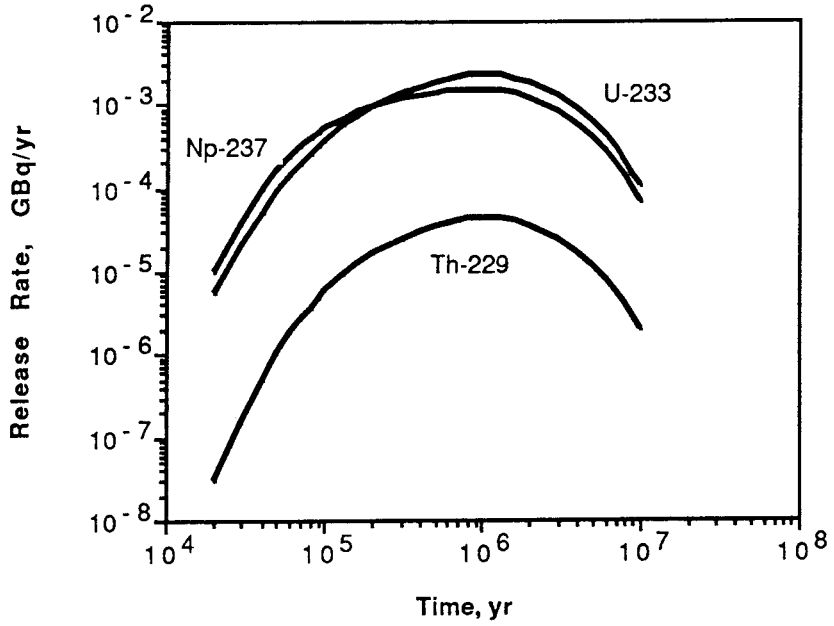

Figure 7-2 Release from the sand-bentonite for the radionuclides in Chain 1 (4N+1).

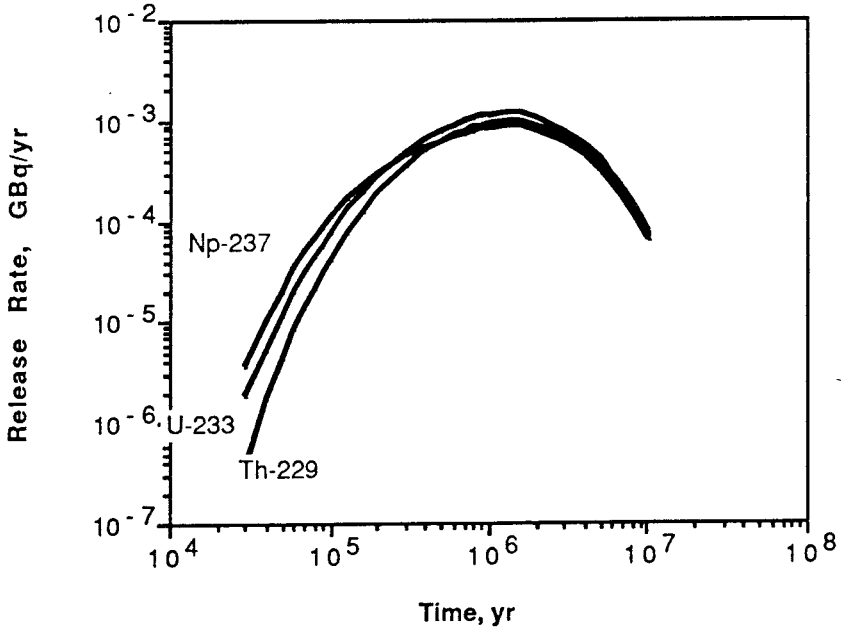

Figure 7-3 Release from the far-field for the radionuclides in Chain 1 (4N+1).

7.1.3 Release of the radionuclides in Chain 2 (4N+3)

Chain 4N+3 includes radionuclide ^{239}Pu as parent and the radionuclides ^{235}U and ^{231}Pa as daughters. The half-lives for these radionuclides are very different which caused some problems in the calculations. The half-lives of ^{239}Pu and ^{231}Pa are short (24,000 and 32,000 years, respectively) while the half-life of ^{235}U is 200 millions years.

The maximum input release (activity/time) for ^{239}Pu is of the same magnitude as the maximum input release for ^{235}U. Due to the ratio between the half-lives, the contribution of ^{239}Pu to the far-field release of ^{235}U is negligible. For this reason the far-field release of ^{235}U and the rest of the chain may be calculated separately. The calculations may be done by using the analytical solution that includes diffusion into the rock matrix and dispersion in the fracture.

The problem is reduced to calculating the far-field release for a two radionuclide chain. Due to the ratio between the half-lives of ^{235}U and ^{231}Pa, we may assume that ^{231}Pa is in equilibrium with ^{235}U, an assumption that is valid for long times. It is expected that the maximum release occurs at a time of about one million years which ensures that the assumption of radioactive equilibrium is fulfilled.

If the release of ^{231}Pa is calculated using the equilibrium condition, the release of ^{235}U may also be calculated using the analytical solution for the advection dispersion equation with matrix diffusion.

The far-field release of these radionuclides is shown in Figures 7-4 and 7-5. The far-field release of ^{239}Pu is reduced to about 16 % of the release from the sand-bentonite barrier. The maximum release for ^{235}U from the far-field is about 70 % of the release from the sand-bentonite barrier. The far-field release of ^{231}Pa is determined by the release of ^{235}U.

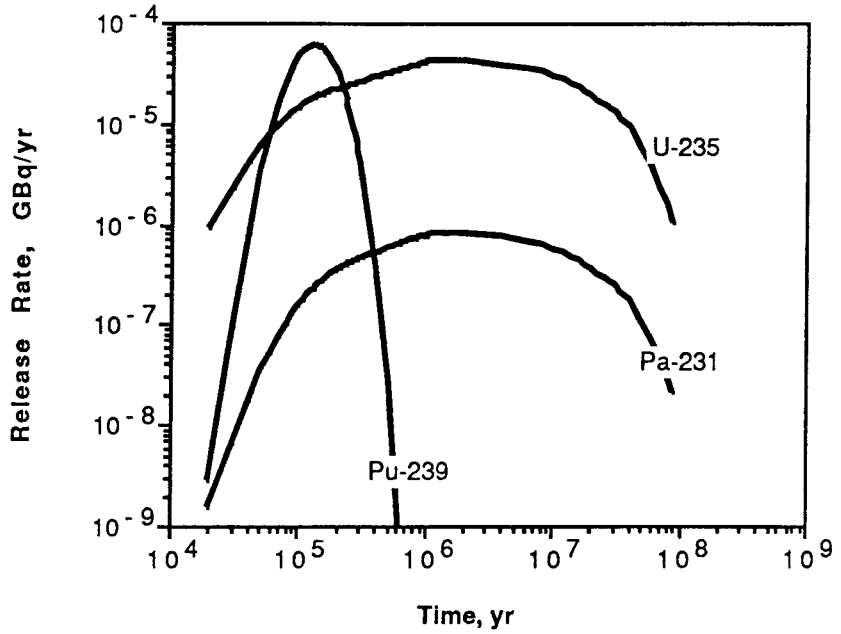

Figure 7-4 Release from the sand-bentonite for the radionuclides in Chain 2 (4N+3).

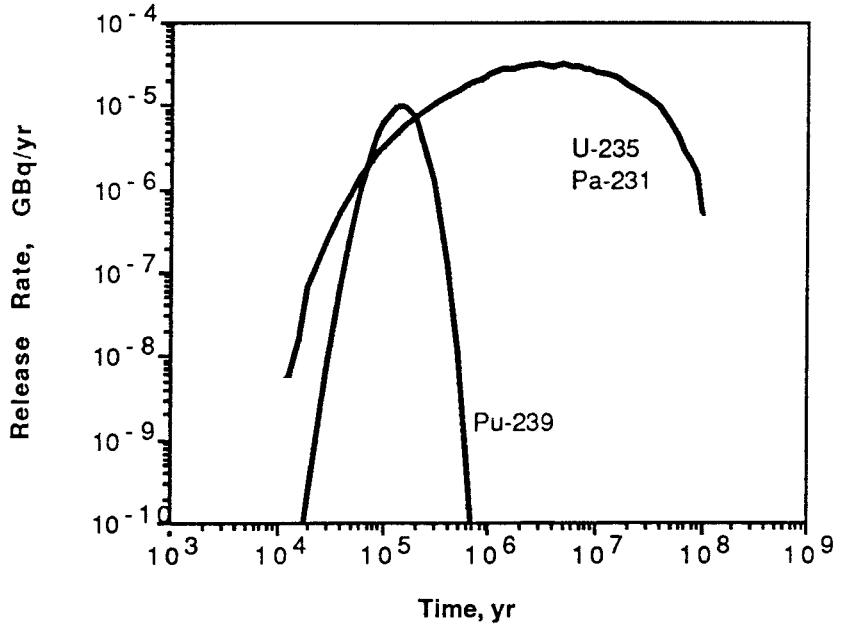

Figure 7-5 Release from the far-field for the radionuclides in Chain 2 (4N+3).

7.1.4 Release of the radionuclides in Chain 3 (4N)

Chain 4N includes the radionuclides ^{240}Pu, ^{236}U, and ^{232}Th. The half-lives of these radionuclides increase with the decay in the chain. For numerical reasons the input release from the sand-bentonite to the far-field is transformed to concentration instead of activity.

The results are shown in Figures 7-6 and 7-7. Release from the far-field for ^{240}Pu is reduced to 9 % of the release from the sand-bentonite barrier. For ^{236}U the release is reduced to about 65 %.

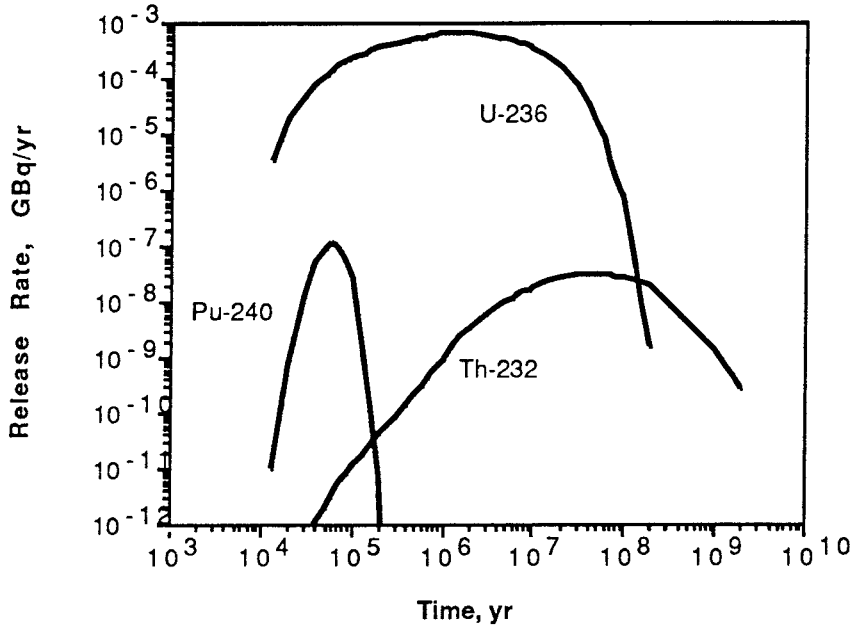

Figure 7-6 Release from the sand-bentonite for the radionuclides in Chain 3 (4N).

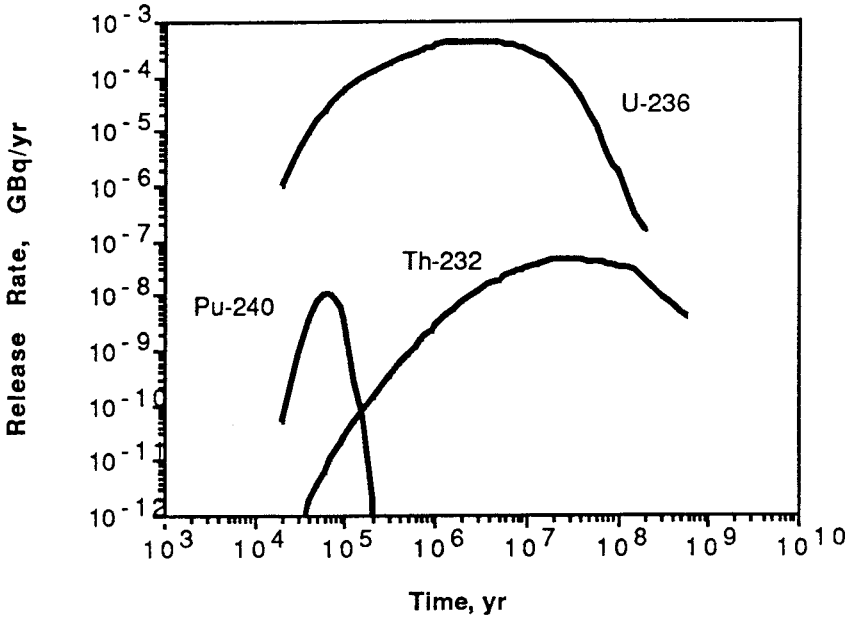

Figure 7-7 Release from the far-field for the radionuclides in Chain 3 (4N).

7.1.5 Release of the radionuclides in Chain 4 (4N+2)

In this chain we study four radionuclides: ^{238}U, ^{234}U, ^{230}Th, and ^{226}Ra. The program TRUCHN was modified to work with four radionuclides. Runs using the four radionuclides require long CPU time due to the short half-life of ^{226}Ra. For this reason a run with the three first radionuclides was carried out. The release of ^{226}Ra is calculated assuming equilibrium between ^{230}Th and ^{226}Ra. The release of ^{234}U is determined principally by its own input, the decay from ^{238}U to ^{234}U is negligible. The results from the latter calculation are shown in Figures 7-8 and 7-9.

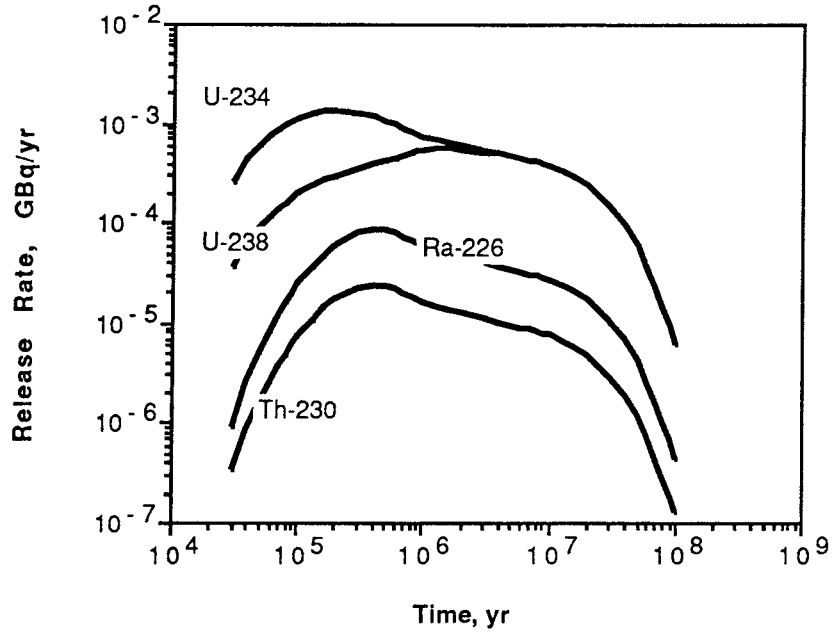

Figure 7-8 Release from the sand-bentonite for the radionuclides in Chain 4 (4N+2).

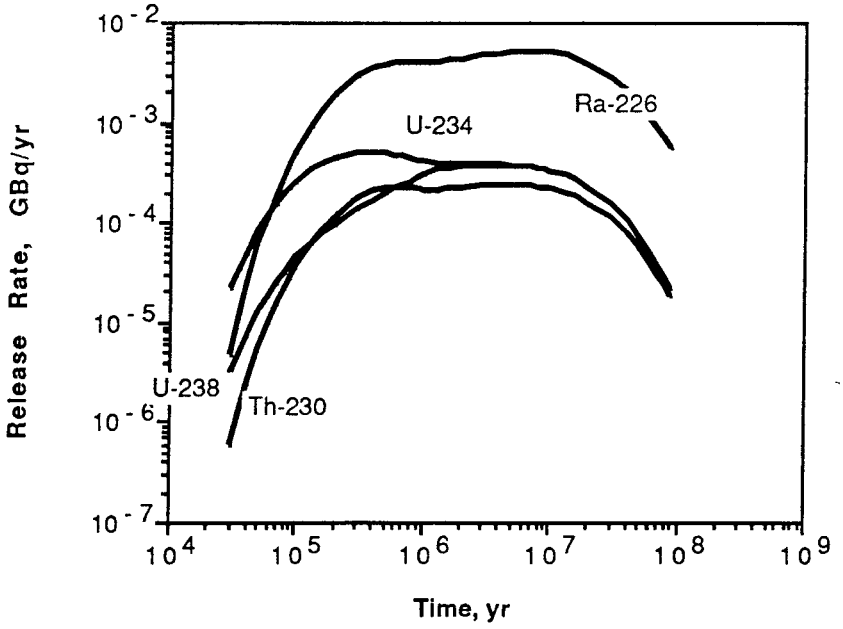

Figure 7-9 Release from the far-field for the radionuclides in Chain 4 (4N+2).

7.1.6 Summary of the release of actinides and daughter nuclides.

The release from the far-field for the different radionuclides are shown in Table 7-1. Figure 7-10 shows the relationship between the release from the near-field and release from the far-field.

The reduction of the release by travel through the far-field is less than an order of magnitude for the parent nuclides and early daughters. The seeming increase of some late daughters is due to the fact that there is little of these nuclides coming directly from the near-field. The main release is generated during the transport through the geosphere.

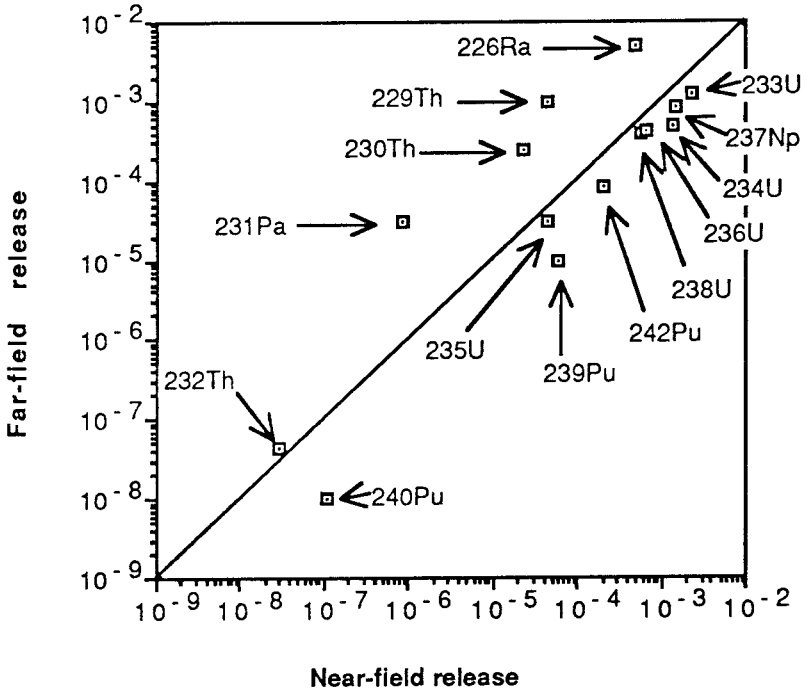

Figure 7-10 Release from the far-field compared with the release from the near-field.

Table 7-1 Release from the near-field and from the far-field.

Nuclides	from near-field release GBq/a	from near-field time a	from far-field release GBq/a	from far-field time a
Chain 1				
^{237}Np	$1.5 \cdot 10^{-3}$	$1.2 \cdot 10^{6}$	$8.8 \cdot 10^{-4}$	$1.3 \cdot 10^{6}$
^{233}U	$2.3 \cdot 10^{-3}$	$1.2 \cdot 10^{6}$	$1.2 \cdot 10^{-3}$	$1.3 \cdot 10^{6}$
^{229}Th	$4.5 \cdot 10^{-5}$	$1.2 \cdot 10^{6}$	$1.0 \cdot 10^{-3}$	$1.3 \cdot 10^{6}$
Chain 2				
^{239}Pu	$6.0 \cdot 10^{-5}$	$1.3 \cdot 10^{5}$	$9.7 \cdot 10^{-6}$	$1.6 \cdot 10^{5}$
^{235}U	$4.4 \cdot 10^{-5}$	$1.2 \cdot 10^{6}$	$3.0 \cdot 10^{-5}$	$3.0 \cdot 10^{6}$
^{231}Pa	$8.3 \cdot 10^{-7}$	$1.2 \cdot 10^{6}$	$3.0 \cdot 10^{-5}$	$3.0 \cdot 10^{6}$
Chain 3				
^{240}Pu	$1.1 \cdot 10^{-7}$	$6.0 \cdot 10^{4}$	$1.0 \cdot 10^{-8}$	$7.0 \cdot 10^{4}$
^{236}U	$6.7 \cdot 10^{-4}$	$1.2 \cdot 10^{6}$	$4.3 \cdot 10^{-4}$	$2.5 \cdot 10^{6}$
^{232}Th	$3.0 \cdot 10^{-8}$	$4.5 \cdot 10^{7}$	$4.4 \cdot 10^{-8}$	$3.0 \cdot 10^{7}$
Chain 4				
^{242}Pu	$2.0 \cdot 10^{-4}$	$6.0 \cdot 10^{5}$	$8.5 \cdot 10^{-5}$	$7.0 \cdot 10^{5}$
^{238}U	$5.7 \cdot 10^{-4}$	$1.2 \cdot 10^{6}$	$3.8 \cdot 10^{-4}$	$4.5 \cdot 10^{6}$
^{234}U	$1.3 \cdot 10^{-3}$	$2.0 \cdot 10^{5}$	$5.1 \cdot 10^{-4}$	$4.0 \cdot 10^{5}$
^{230}Th	$2.3 \cdot 10^{-5}$	$4.2 \cdot 10^{5}$	$2.4 \cdot 10^{-4}$	$5.0 \cdot 10^{6}$
^{226}Ra	$8.3 \cdot 10^{-5}$	$4.2 \cdot 10^{5}$	$5.0 \cdot 10^{-3}$	$6.0 \cdot 10^{6}$

7.2 RELEASE OF NUCLIDES WHICH ARE CONCENTRATION LIMITED BY SOLUBILITY

In the previous calculations, it was assumed that the concentration around the canister is determined by the rate of release of the radionuclides determined by the rate of dissolution of the uranium-dioxide matrix of the fuel. The total time for this dissolution is about 1,200,000 years. In the canister there are oxidizing conditions, but the redox conditions outside the canister are reducing. In the latter case the solubility of some radionuclides is strongly reduced.

The release from the far-field of the radionuclides in Chain 4 is calculated limiting the concentration around the canister to the solubility. The solubility for the nuclides was taken to be $1 \cdot 10^{-5}$ kg/m^3 for U and $4 \cdot 10^{-7}$ kg/m^3 for Th /Lindgren and Skagius, 1988/. In this case the release to the biosphere is reduced by about three orders of magnitude. The results are shown in Table 7-2. Figure 7-11 shows the release from the sand-bentonite barrier to the far-field. The release from the far-field is shown in Figure 7-12.

Table 7-2 Release from the far-field for the concentration around the canister limited by the solubility under reducing conditions.

Nuclides	Release, GBq/a	
	Reference	Solubility limited
Chain 4		
^{238}U(1)	$3.8 \cdot 10^{-4}$	$1.2 \cdot 10^{-7}$
^{234}U(1)	$5.1 \cdot 10^{-4}$	$2.1 \cdot 10^{-7}$
^{230}Th(2)	$2.4 \cdot 10^{-4}$	$1.0 \cdot 10^{-7}$
^{226}Ra(2)	$5.0 \cdot 10^{-3}$	$3.0 \cdot 10^{-6}$

(1) Release calculated for only one nuclide.
(2) Release estimated.

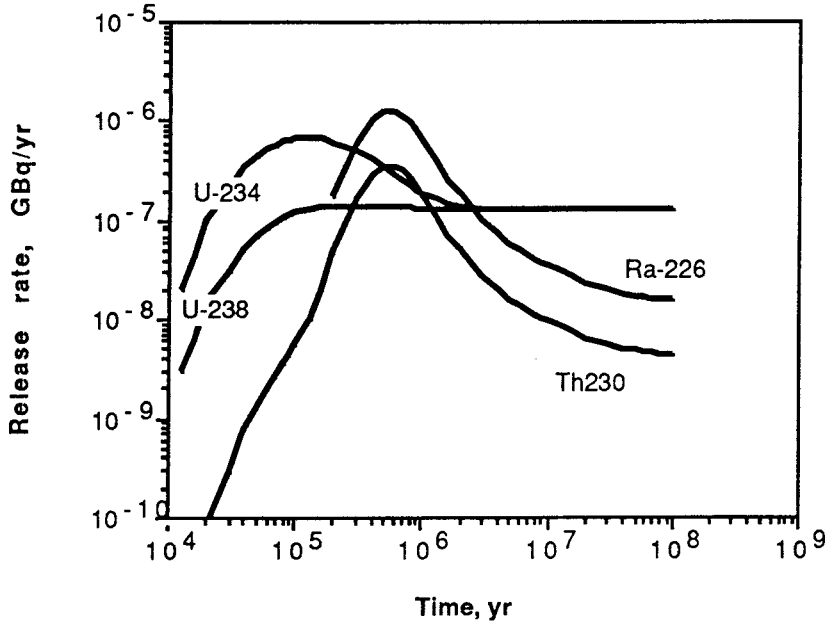

Figure 7-11 Release from the sand-bentonite for the radionuclides in Chain 4 (4N+2). Concentration outside the canister is limited by solubility.

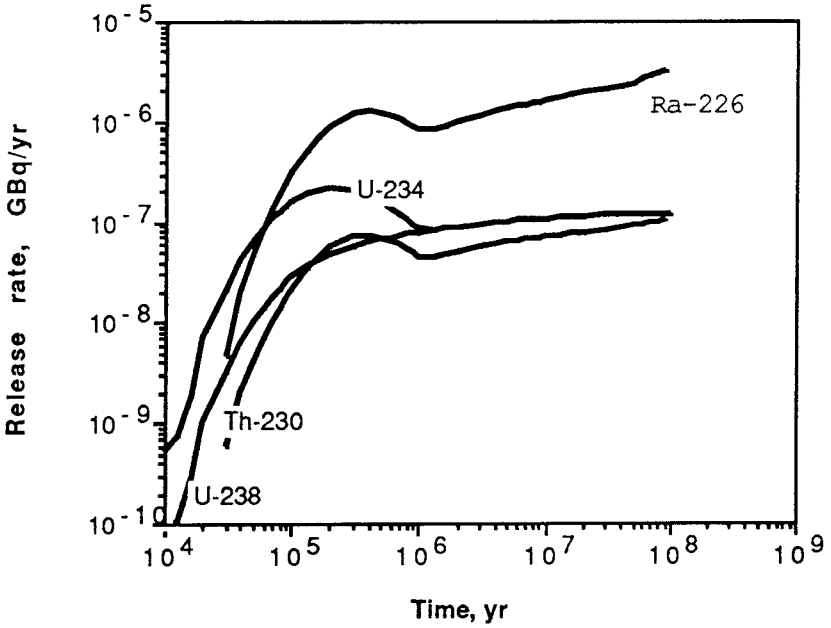

Figure 7-12 Release from the far-field for the radionuclides in Chain 4 (4N+2). Concentration outside the canister is limited by solubility.

7.3 RESULTS OF VARIATION CASES

In the calculations above, we have used a reference case. In this reference case the transport distance used is 100 m. A distance of about 100 m may be found if an upward groundwater flow exists around the repository. If the flow is horizontal or downward the transport distance may be much longer before the radionuclides reach the biosphere. The distance may be several hundreds of meters up to kilometers.

The sorption coefficients used for the radionuclides are 5.0 m^3/kg with the exception of the coefficient for Ra, in which 0.1 m^3/kg is used. These values are for reducing conditions. Uranium may have, in some cases, a value of 1.0 m^3/kg for its sorption coefficient. Moreover if oxidizing conditions exist in the groundwater that will transport the radionuclides outside the sand-bentonite barrier, then some sorption coefficients may be strongly changed. In this case Np has a sorption coefficient of 0.1 m^3/kg and U a value of 0.05 m^3/kg.

7.3.1 Release for other transport distances

The transport distance in the reference case is 100 m. As discussed above this distance may be longer if the flow is downward and horizontal. Calculations are made for transport distances of 400 and 1600 m. The release is calculated using an analytical solution in the cases in which this is possible and estimated in the other cases. The results are shown in Table 7-3.

Table 7-3 Maximum release from the far-field for different transport distances.

Nuclides	Release, GBq/a		
	Reference 100 m	400 m	1600 m
Chain 1			
^{237}Np	$8.8 \cdot 10^{-4}$	$4.1 \cdot 10^{-4}$	$6.5 \cdot 10^{-5}$
^{233}U	$1.2 \cdot 10^{-3}$	$4.6 \cdot 10^{-4}$	$6.8 \cdot 10^{-5}$
^{229}Th	$1.0 \cdot 10^{-3}$	$4.5 \cdot 10^{-4}$	$6.6 \cdot 10^{-5}$
Chain 2			
^{239}Pu (1)	$9.7 \cdot 10^{-6}$	$1.4 \cdot 10^{-6}$	$2.1 \cdot 10^{-8}$
^{235}U (1)	$3.0 \cdot 10^{-5}$	$1.8 \cdot 10^{-5}$	$8.0 \cdot 10^{-6}$
^{231}Pa (2)	$3.0 \cdot 10^{-5}$	$1.8 \cdot 10^{-5}$	$8.0 \cdot 10^{-6}$
Chain 3			
^{240}Pu (1)	$1.0 \cdot 10^{-8}$	$1.1 \cdot 10^{-9}$	$1.0 \cdot 10^{-11}$
^{236}U (1)	$4.3 \cdot 10^{-4}$	$2.4 \cdot 10^{-4}$	$9.4 \cdot 10^{-5}$
^{232}Th (1)	$4.4 \cdot 10^{-8}$	$3.1 \cdot 10^{-8}$	$1.8 \cdot 10^{-8}$
Chain 4			
^{242}Pu (1)	$8.5 \cdot 10^{-5}$	$3.5 \cdot 10^{-5}$	$6.2 \cdot 10^{-6}$
^{238}U (1)	$3.8 \cdot 10^{-4}$	$2.4 \cdot 10^{-4}$	$1.0 \cdot 10^{-4}$
^{234}U (1)	$5.1 \cdot 10^{-4}$	$1.4 \cdot 10^{-4}$	$7.7 \cdot 10^{-5}$
^{230}Th (2)	$2.4 \cdot 10^{-4}$	$6.6 \cdot 10^{-5}$	$3.6 \cdot 10^{-5}$
^{226}Ra (2)	$5.0 \cdot 10^{-3}$	$1.4 \cdot 10^{-3}$	$7.5 \cdot 10^{-4}$

(1) Release calculated for only one nuclide.
(2) Release estimated.

7.3.2 Release for other sorption coefficients

The sorption coefficient for U is, in some cases, estimated to be 1.0 m^3/kg instead of 5.0 m^3/kg (see Table 4-1). For oxidizing conditions the sorption coefficient for U is 0.05 m^3/kg and for Np 0.1 m^3/kg. This modifies the release of these radionuclides and of its daughters. Simple calculations are made to estimate the magnitude of these changes. The release of the most important radionuclides are calculated using an analytical solution. From these values an estimate is made for the release of the other radionuclides. Table 7-4 shows the release from the far-field for reducing and oxidizing conditions.

The calculations for reducing conditions of the nuclides of Chain 4 are performed using the value of 1.0 m^3/kg for the sorption coefficient of U.

Table 7-4 Release from the far-field.

Nuclides	Release, GBq/a Reference case	Reducing conditions	Oxidizing conditions
Chain 1			
^{237}Np (1)	$8.8 \cdot 10^{-4}$	-	$1.4 \cdot 10^{-3}$
^{233}U (2)	$1.2 \cdot 10^{-3}$	-	$3.0 \cdot 10^{-3}$
^{229}Th (2)	$1.0 \cdot 10^{-3}$	-	$1.2 \cdot 10^{-3}$
Chain 2			
^{239}Pu (1)	$9.7 \cdot 10^{-6}$	-	$9.7 \cdot 10^{-6}$
^{235}U (2)	$3.0 \cdot 10^{-5}$	-	$4.1 \cdot 10^{-5}$
^{231}Pa (2)	$3.0 \cdot 10^{-5}$	-	$2.1 \cdot 10^{-5}$
Chain 3			
^{240}Pu (1)	$1.0 \cdot 10^{-8}$	-	$1.0 \cdot 10^{-8}$
^{236}U (1)	$4.3 \cdot 10^{-4}$	-	$6.0 \cdot 10^{-4}$
^{232}Th (1)	$4.4 \cdot 10^{-8}$	-	$5.4 \cdot 10^{-8}$
Chain 4 (3)			
^{238}U (1)	$3.8 \cdot 10^{-4}$	$1.1 \cdot 10^{-3}$	$1.2 \cdot 10^{-3}$
^{234}U (1)	$5.1 \cdot 10^{-4}$	$1.8 \cdot 10^{-3}$	$2.6 \cdot 10^{-3}$
^{230}Th (2)	$2.4 \cdot 10^{-4}$	$3.6 \cdot 10^{-4}$	$1.2 \cdot 10^{-3}$
^{226}Ra (2)	$5.0 \cdot 10^{-3}$	$7.6 \cdot 10^{-3}$	$2.5 \cdot 10^{-2}$

(1) Release calculated for only one nuclide.
(2) Release estimated.
(3) Release calculated using a sorption coefficient of 1.0 m^3/kg for U, for reducing conditions.

8 DISCUSSION AND CONCLUSIONS

8.1 APPLICABILITY OF MODEL CONCEPT

Experimental observations indicate that water flows very unevenly distributed in crystalline rock. Water flows in channels of different widths and with different flowrates. Two channeling concepts were compared in these calculations: (a) separate channels transport the water and radionuclides without connections to other channels (channeling model) and (b) the water and radionuclides are transported by channels which mix their water many times along their paths (mixing model). It may be expected that for short distances with a low channel frequency the number of mixings is small or nonexistent. For zones with a high channel frequency mixing may be expected to be important if the radionuclides are transported over long distances. The calculations showed that for a given contact surface the mixing case will give lower effluent concentrations.

The proposed hydraulic cage surrounding the repository has been neglected in the calculations presented in this report. The effect of the hydraulic cage is discussed in other report (SKB, 1989)

8.2 APPLICABILITY OF DATA

There are only a few investigations where the type of observations which give data for use in a channeling model have been presented. We have therefore used the SFR data which are the best available at present.

As discussed previously, the model parameters were tested to determine which influenced the contamination from the repository most. These entities are the sorption capacity of the rock matrix, the surface area of the channels, and the water flowrate or water flux.

The sorption coefficient is usually determined in the laboratory. The values found for a given radionuclide vary with rock type. Moreover the sorption coefficient may differ in the same kind of rock. On the other hand this is the parameter which requires less accuracy in its determination. This is

because a change by a factor of 10 in this parameter is equivalent to a change by a factor of 3.15 in the other parameters. The same also applies for the diffusivity in the rock matrix.

The width of the channels is difficult to determine for a given rock mass. For the rock around a drift the information available is only the trace of the fracture on the drift wall. The width of the channels observed on the surface of the drift may be influenced by the presence of the drift itself. A quantitative description is very complicated. There are channels which have a high flowrate and are very narrow. In this case the retardation is small or negligible even for nuclides with large sorption coefficients because of the small surface from which the nuclides may diffuse into the rock matrix.

The water flowrate was obtained from a survey of site areas around Sweden. If the flowrate is increased by a factor of 10, the release rates of the nonsorbing nuclides increase about a factor of 3 from the near-field. The transport in the far-field is not influenced for those that were not decaying for the lower flowrate, whereas those that decayed will be given less time to decay.

The investigation of the channel aperture showed that for the times of interest it has little or no impact on the radionuclide concentration.

8.3 COMMENTS ON THE RESULTS

The results show that the retardation and decay of the radionuclides in the far-field are not important in the reference case. The maximum release is reduced, in some cases, to about 50 % for a transport distance of 100 m. The value is somewhat smaller for radionuclides with shorter half-lives. For long lived radionuclides the release is almost equal to the release from the near-field.

For larger transport distances, of about one km, the release may be significantly reduced. For this larger distance, it is also expected that there may exist a certain mixing between the channels. Mixing between channels with different properties (different flowrate) significantly reduces the release of radionuclides in the far-field.

In the release calculations, it was assumed that the sorption coefficient for the radionuclides considered is 5.0 m^3/kg. U may in some cases have a value of 1.0 m^3/kg. In this case the release of U and its daughters is increased and the effect of the

far-field is negligible. The same situation is found if it is considered that oxidizing conditions exist in the groundwater outside the sand-bentonite barrier.

In the reference case, the limited solubility of the radionuclides under reducing conditions outside the canister are not taken into account. When the solubility limits of the radionuclides under reducing conditions are used, the releases from the near- and far-field are strongly reduced.

The flow distribution and channeling observations upon which this paper is based are very recent and indicate that there may be less wetted surface in the rock than previously thought. The models are also new and have not been extensively applied. The presented results are thus based on new observations, interpretations, and models.

NOTATION

a	Specific surface	m^2/m^3
c	Concentration in the liquid	mol/m^3
c_f	Concentration in the liquid in the fracture	mol/m^3
c_o	initial concentration	mol/m^3
c_p	Concentration in the liquid in the pores	mol/m^3
D_a	Apparent diffusion coefficient	m^2/s
D_e	Effective diffusion coefficient	m^2/s
D_L	Dispersion coefficient	m^2/s
H	Hydraulic head	m
K_a	Surface sorption coefficient	m
K_d	Mass sorption coefficient	m^3/kg
K_p	Hydraulic conductivity	m/s
L	Length	m
Q	Flowrate	m^3/s
R_a	Surface retardation factor	-
S	Fracture spacing	m
t	Time	s
t_w	Water residence time	s
u	Water velocity	m/s
u_N	Nuclide transport velocity	m/s
u_o	Darcy velocity	$m^3/m^2 \cdot s$
W	Channel width	m
x	Distance into the rock from a fracture	m
z	Distance in the direction of the flow	m
δ	Fracture aperture	m
λ	Decay constant	s^{-1}
ρ_p	Density of rock matrix	kg/m^3

REFERENCES

Bergström, U., and S. Nordlinder, "SKB-WP-CAVE Project, Individual radiation doses from nuclides containing in a WP-repository for spent fuel, SKB Technical Report TR 89-06, 1989.

Bolvede, P., and R. Christiansson, "SKB Forsmarksarbetena SFR. Vattenförande Sprickor inom Lageområdet", VIAK, Stockholm (1987). (in Swedish) (Water bearing fractures in the repository area.)

Lindgren, M., and K. Skagius, "SKB-WP-CAVE Project, Radionuclide release from the bentonite-sand barrier in a Wp-Cave repository," SKB Technical Report TR 89-04, 1989.

Neretnieks, I., "Diffusion in the Rock Matrix: An Important Factor in Radionuclide Retardation?", J. Geophys. Res. 85, p 4379-4397 (1980).

Neretnieks, I., "Transport in fractured rocks", Proceedings, Memoires of the 17th International Congress of IAH, Tucson, AZ, Vol. XVII, p 301-318 (1985).

Neretnieks, I., T. Eriksen, and P. Tähtinen, "Tracer Movement in a Single Fissure in Granitic Rock: Some Experimental Results and their Interpretation", Water Resour. Res. 18, p 849-858 (1982).

Neretnieks, I., H. Abelin, and L. Birgersson, "Some recent observations of channeling in fractured rocks. Its potential impact on radionuclide migration.," In DOE/AECL conference sept 15-17, 1987, San Francisco, proceedings, 1987.

Palmqvist K., Stanfors R. "The Kymmen power station TBM tunnel. Hydrogeological mapping and analysis." SKB Technical report 87-26, 1987.

Rasmuson, A., "Analysis of hydrodynamic dispersion in discrete fracture networks using the method of moments", Water Resour. Res. 21, p 1677-1683 (1985).

Rasmuson, A., A. Bengtsson, B. Grundfelt, and I. Neretnieks, "Radionuclide chain migration in fissured rock - The influence of matrix diffusion," KBS Technical Report TR 82-04, 1982.

Skagius, K., A. Bengtsson, and M. Lindgren, "SKB-WP-CAVE Project, Release of fission and activation products from the bentonite-sand barrier in a WP-Cave repository," SKB Progress Report AR 88-14.

SKB-WP-CAVE Project, Some notes on technical issues, SKB Technical Report TR 89-07, 1989.

APPENDIX A. RELEASE RATE PLOTS

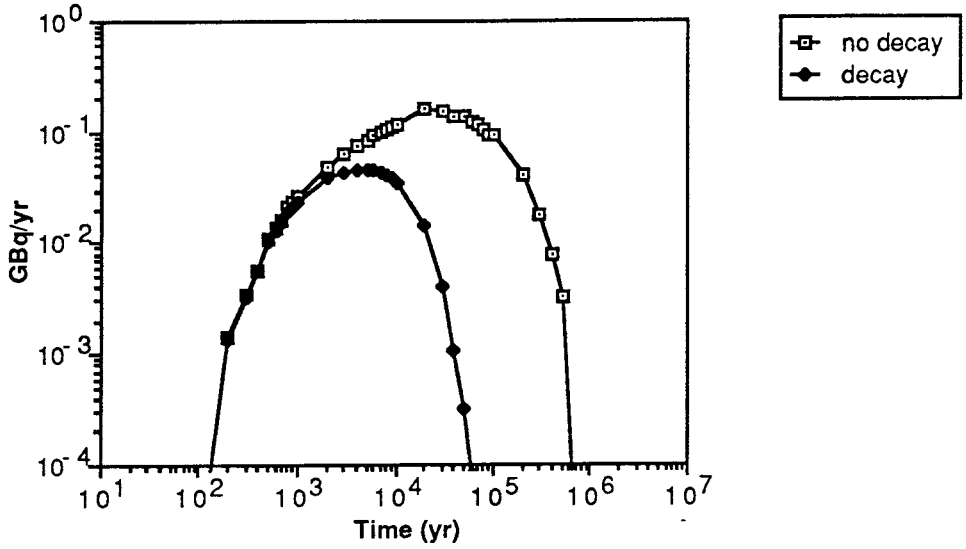

Figure A-1 Release rates of ^{14}C from the far-field to the biosphere.

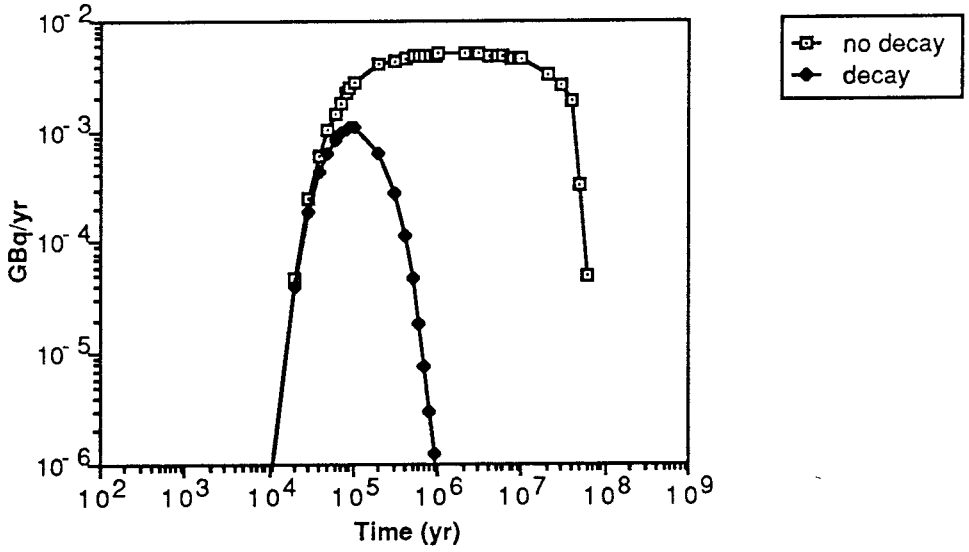

Figure A-2 Release rates of ^{59}Nb from the far-field to the biosphere.

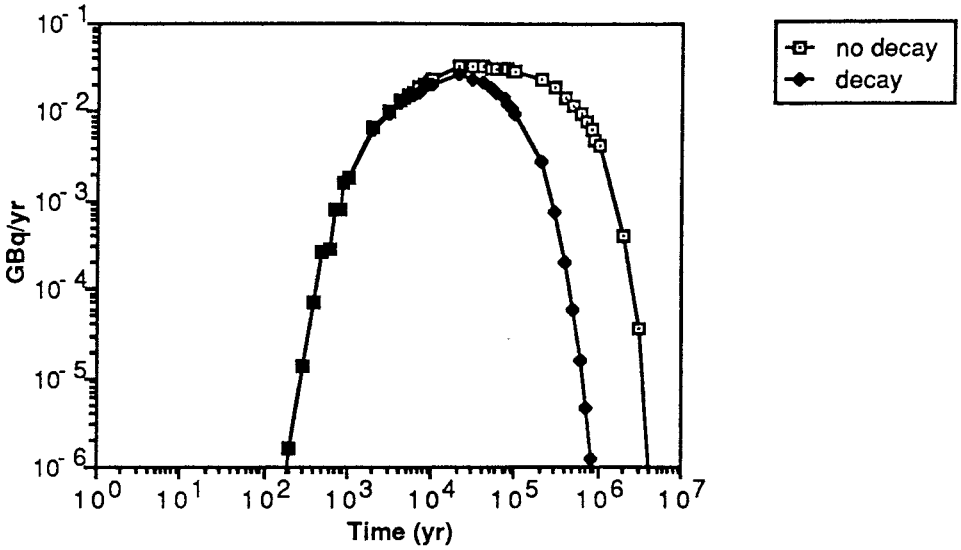

Figure A-3 Release rates of ^{79}Se from the far-field to the biosphere.

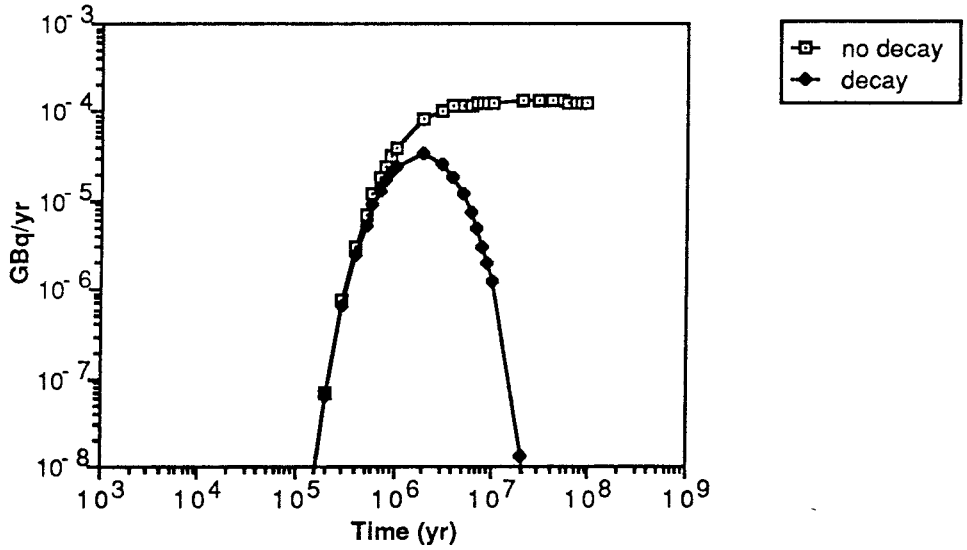

Figure A-4 Release rates of ^{93}Zr from the far-field to the biosphere.

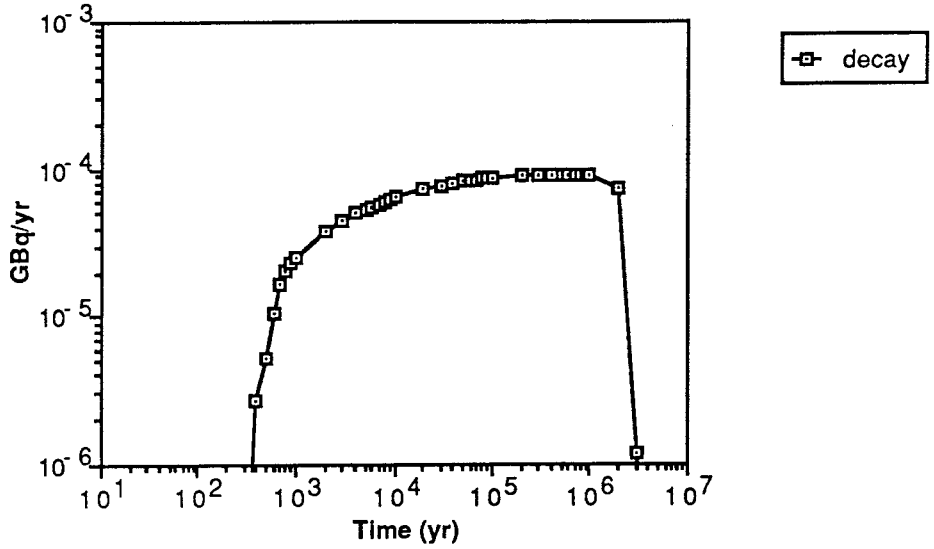

Figure A-5 Release rate of ^{99}Tc from the far-field to the biosphere.

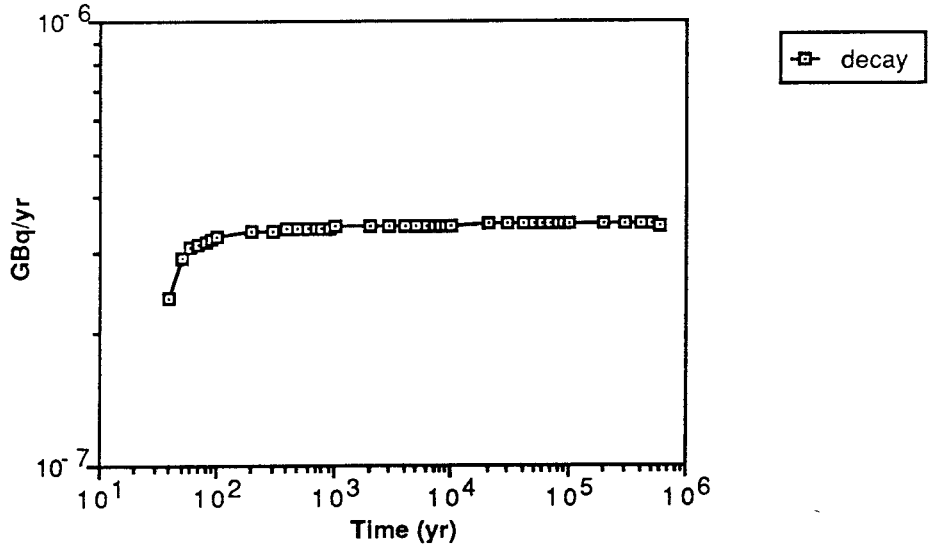

Figure A-6 Release rate of ^{107}Pd from the far-field to the biosphere.

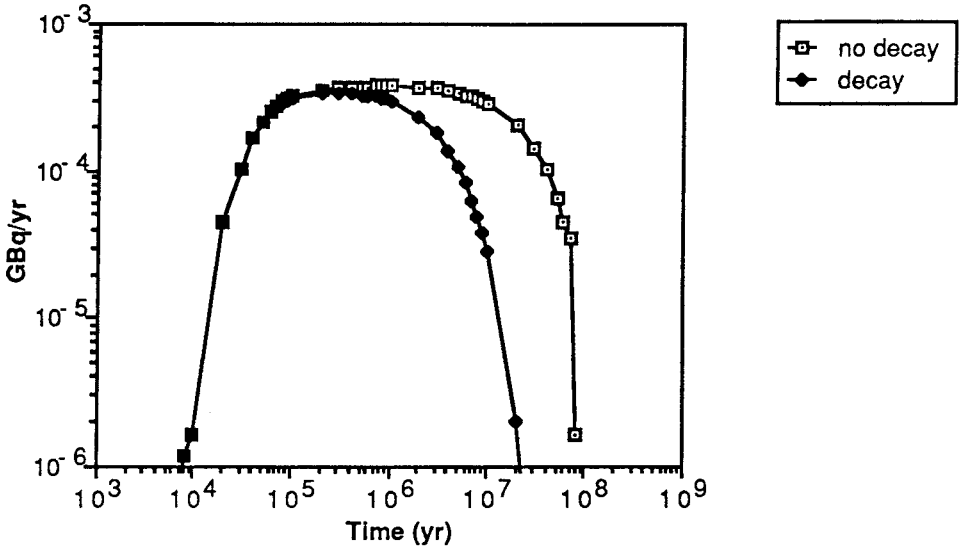

Figure A-7 Release rates of ^{135}Cs from the far-field to the biosphere.

APPENDIX B. PRELIMINARY TESTS PERFORMED WITH TRUCHN

Some preliminary tests were performed with the numerical code TRUCHN to determine an adequate grid. The fracture and the rock matrix in the direction of the flow are divided in nodes with the same length. In the fracture, advection is more important than dispersion.

The nodes in the rock matrix in the direction perpendicular to the flow were defined with sizes increasing from the fracture. This is due to that the transport in the rock matrix occurs by diffusion. The release rate from the sand-bentonite varies in a wide interval (several order of magnitude), this was anticipated to cause problem in the numerical stability of the code.

MIGRATION INTO THE ROCK MATRIX

TRUCHN computer runs were performed using the radionuclide ^{239}Pu to determine the sizes of the nodes in the rock matrix. We define as criterion for the penetration length, that the concentration in the far-away nodes is 0.05 C_o. The penetration length may be evaluated analytically /Neretnieks, 1980/. ^{239}Pu is chosen as an example due to that most of the radionuclides are highly sorbing substances. For ^{239}Pu the penetration length is about 3 cm for a time of one million years. The properties used in the calculations are as follows:

$K_d = 5\ m^3/kg$
$D_e = 5 \cdot 10^{-14}\ m^2/s$
$\rho_p = 2700\ kg/m^3$
$c_o = 1$
Pe = 10
decay = none.

From knowing the maximum penetration distance, the TRUCHN program was tested to determine the optimal node size. The release rates for ^{239}Pu for the different node sizes tested were compared to the release rate calculated using an analytical solution.
It was observed that to obtain good results from TRUCHN, a small size of the nodes closest to the channel surface was required. Two sizes for the node

closest to the channel were finally decided upon, 0.1 mm and 0.01 mm. Both values gave good results in comparison to the analytical results with the exception of the 0.1 mm size at earlier times. The results for the two size increments and the analytical results are shown in Figure C-1. Even though the 0.1 mm size concentrations are larger at earlier times, the required computer time to calculate for six channels to one million years was about 3.5 hours. Comparing this result to the 0.01 mm case, the 0.01 mm size case requires a computer time 3 to 4 times longer. Knowing the capabilities of each size case, one can use a combination of the two cases to obtain good results at an early time by using the 0.01 mm case and thus finishing the calculations using the 0.1 mm case.

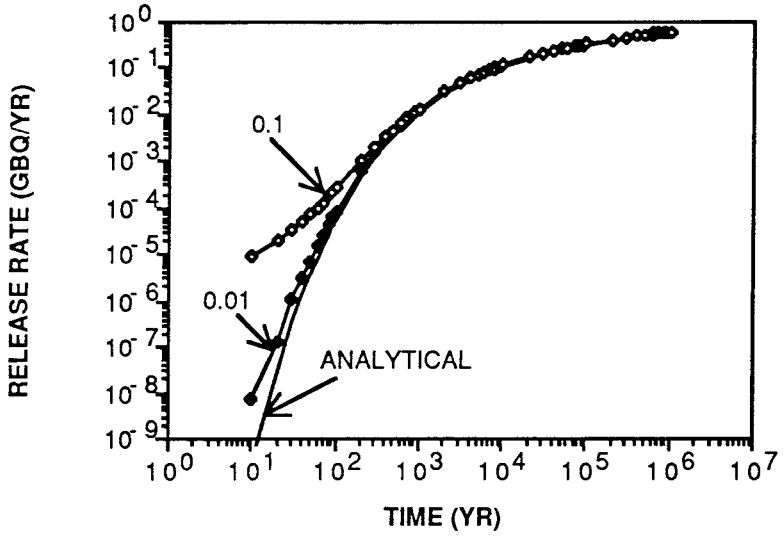

Figure C-1 Comparison of the release rates for the radionuclide ^{239}Pu between the two TRUCHN runs with 0.1 mm and 0.01 mm for the node closest to the fracture, and the analytical results.

APPENDIX C. TREATMENT OF VARIABLE INPUT DATA TO TRUCHN

The data files received from KEMAKTA contain the radionuclides release rates in GBq/a at specific time periods. For some nuclides, all the release rates are at very low levels. This causes difficulties for the TRUCHN program. For this reason, all the input data files were scaled whereby the maximum release rate was set to one and all the other release rates scaled with this maximum value. However, this procedure does not eliminate the very low release rate values which may occur at the earlier or later time periods. In most cases, these values are of little importance and thus can be neglected in the calculations. These values were handled by eliminating any that were lower than a designated cut-off value. In our case, the cut-off value was $1 \cdot 10^{-4}$.

A program was written to perform the above calculations. The output from this program can be directly transfered into the input data file. Once the calculations from TRUCHN are completed, the output is read into another Fortran program which converts the final release rates back to their actual release rate levels.

List of SKB reports

Annual Reports

1977–78
TR 121
KBS Technical Reports 1 – 120.
Summaries. Stockholm, May 1979.

1979
TR 79–28
The KBS Annual Report 1979.
KBS Technical Reports 79-01 – 79-27.
Summaries. Stockholm, March 1980.

1980
TR 80–26
The KBS Annual Report 1980.
KBS Technical Reports 80-01 – 80-25.
Summaries. Stockholm, March 1981.

1981
TR 81–17
The KBS Annual Report 1981.
KBS Technical Reports 81-01 – 81-16.
Summaries. Stockholm, April 1982.

1982
TR 82–28
The KBS Annual Report 1982.
KBS Technical Reports 82-01 – 82-27.
Summaries. Stockholm, July 1983.

1983
TR 83–77
The KBS Annual Report 1983.
KBS Technical Reports 83-01 – 83-76
Summaries. Stockholm, June 1984.

1984
TR 85–01
Annual Research and Development Report 1984
Including Summaries of Technical Reports Issued during 1984. (Technical Reports 84-01– 84-19)
Stockholm June 1985.

1985
TR 85-20
Annual Research and Development Report 1985
Including Summaries of Technical Reports Issued during 1985. (Technical Reports 85-01-85-19)
Stockholm May 1986.

1986
TR 86-31
SKB Annual Report 1986
Including Summaries of Technical Reports Issued during 1986
Stockholm, May 1987

1987
TR 87-33
SKB Annual Report 1987
Including Summaries of Technical Reports Issued during 1987
Stockholm, May 1988

1988
TR 88-32
SKB Annual Report 1988
Including Summaries of Technical Reports Issued during 1988
Stockholm, May 1989

Technical Reports

1989
TR 89-01
Near-distance seismological monitoring of the Lansjärv neotectonic fault region Part II: 1988
Rutger Wahlström, Sven-Olof Linder,
Conny Holmqvist, Hans-Edy Mårtensson
Seismological Department, Uppsala University,
Uppsala
January 1989

TR 89-02
Description of background data in SKB database GEOTAB
Ebbe Eriksson, Stefan Sehlstedt
SGAB, Luleå
February 1989

TR 89-03
Characterization of the morphology, basement rock and tectonics in Sweden
Kennert Röshoff
August 1988

TR 89-04
SKB WP-Cave Project
Radionuclide release from the near-field in a WP-Cave repository
Maria Lindgren, Kristina Skagius
Kemakta Consultants Co, Stockholm
April 1989